Front. Phys. 11(4), 110309 (2016)
DOI 10.1007/s11467-016-0570-9

REVIEW ARTICLE

Stochastic description of quantum Brownian dynamics

Yun-An Yan[1,*], **Jiushu Shao**[2,†]

[1] *Guizhou Provincial Key Laboratory of Computational Nano-Material Science, Guizhou Education University, Guizhou 550018, China*
[2] *Center of Advanced Quantum Studies and College of Chemistry, Beijing Normal University, Beijing 100875, China*
*Corresponding authors. E-mail: *yunan@gznc.edu.cn, †jiushu@bnu.edu.cn*
Received February 20, 2016; Accepted March 14, 2016

Classical Brownian motion has well been investigated since the pioneering work of Einstein, which inspired mathematicians to lay the theoretical foundation of stochastic processes. A stochastic formulation for quantum dynamics of dissipative systems described by the system-plus-bath model has been developed and found many applications in chemical dynamics, spectroscopy, quantum transport, and other fields. This article provides a tutorial review of the stochastic formulation for quantum dissipative dynamics. The key idea is to decouple the interaction between the system and the bath by virtue of the Hubbard-Stratonovich transformation or Itô calculus so that the system and the bath are not directly entangled during evolution, rather they are correlated due to the complex white noises introduced. The influence of the bath on the system is thereby defined by an induced stochastic field, which leads to the stochastic Liouville equation for the system. The exact reduced density matrix can be calculated as the stochastic average in the presence of bath-induced fields. In general, the plain implementation of the stochastic formulation is only useful for short-time dynamics, but not efficient for long-time dynamics as the statistical errors go very fast. For linear and other specific systems, the stochastic Liouville equation is a good starting point to derive the master equation. For general systems with decomposable bath-induced processes, the hierarchical approach in the form of a set of deterministic equations of motion is derived based on the stochastic formulation and provides an effective means for simulating the dissipative dynamics. A combination of the stochastic simulation and the hierarchical approach is suggested to solve the zero-temperature dynamics of the spin-boson model. This scheme correctly describes the coherent-incoherent transition (Toulouse limit) at moderate dissipation and predicts a rate dynamics in the overdamped regime. Challenging problems such as the dynamical description of quantum phase transition (localization) and the numerical stability of the trace-conserving, nonlinear stochastic Liouville equation are outlined.

Keywords stochastic description, quantum dissipation, spin-boson model, hierarchical approach

PACS numbers 03.65.Yz, 02.70.-c, 05.30.-d, 05.10.Gg

Contents

*Special Topic: Progress in Open Quantum Systems: Fundamentals and Applications.

1 Introduction

If one would calculate the dynamics of the universe microscopically by either classical or quantum mechanics, one would have an exact solution to the evolution of the universe as a whole and also for any physical variables. This is, of course, an impossible task. Exact simulation with quantum dynamics is subject to the curse

of dimensionality, a term borrowed from Bellman [1]. In fact, as the computer memory required to store the wave function in the Schrödinger picture or the CPU time to propagate the wavefunction by virtue of the path integral grow exponentially with the size of the system, the curse of dimensionality is unavoidable and the exact simulation with quantum dynamics is limited to systems with few degrees of freedom. By contrast, the computational cost with molecular dynamics based on classical mechanics is linearly proportional to the size of the system. Consequently, the molecular dynamics simulation has become a popular and powerful tool for studying physical properties of complex molecular systems when the quantum effect is negligible [2]. However, even linear scaling is too expansive for the simulation of the whole universe or any macroscopic system. Fortunately, we are in general interested in the dynamical behavior of "few" variables instead of the whole universe [3]. These variables, therefore, define the system of interest and the rest of the universe coupled to the system is usually called environment or heat bath.

When a system of interest is coupled to the other perhaps infinite variables, it is a dissipative or open system. Open systems are ubiquitous in the real world because innumerable dynamical processes are mediated by the environmental condensed phases [4–7]. Of most importance are diversified transport phenomena in gases, liquids and solids, chemical reactions in solutions, surfaces or interfaces, biological processes in cells and so on.

A paradigm of open systems is the Brownian particle. In his miracle year of 1905, Einstein laid the physical foundation of the Brownian motion in terms of the Einstein–Smoluchowski relation [8, 9], the precursor of the more general fluctuation-dissipation theorem [10–12]. After the pioneering work of Einstein many scientists have made significant contributions to this field and the culminating results include the Johnson-Nyquist theorem [13, 14], the Langevin equation [15, 16], the Fokker-Planck equation [17–20], the Ornstein–Uhlenbeck process [21], the Kramers problem [22, 23], and the phenomenological stochastic model for lineshape in spectroscopy [24].

Although various open system dynamics have been extensively investigated at different levels, an apparent obstacle in developing a microscopic description is the quantum effect, which becomes even dominant when the temperature of the environment is lower than the scale of the intrinsic energy. The proof of the quantum fluctuation-dissipation theorem was a milestone in the study of quantum Brownian motion [25, 26]. Up to date, there are still no reliable approaches for simulating the quantum dynamics of general open systems. Formally, one can employ the projection operator technique to solve the motion of the bath. By doing so, one obtains the Nakajima-Zwanzig equation which is a generalization of the master equation and contains an extremely complicated retarded time integration over the history of the reduced system [27, 28]. The Langevin equation can be also generalized to deal with the quantum dissipation when the quantum noise is used instead of the classical c-number noise [29]. There have been several excellent monographs and reviews covering quantum Brownian motion [30–34].

A widely used, generic model for describing open systems has been proposed by Caldeira and Leggett [35]. In this model the bath consists of infinite "effective" harmonic oscillators that are linearly coupled to the system and the impact of the bath on the system is fully characterized by its spectral density function. To study the quantum dissipative dynamics, Caldeira and Leggett explored and popularized the path integral influence functional technique originally suggested by Feynman and Vernon [35, 36]. For the Caldeira–Leggett model the influence functional assumes a Gaussian functional form and Feynman first recognized that its real part can be constructed with a Gaussian colored noise [36]. With the same reasoning, Cao and co-workers introduced that the average over the degrees of freedom of the bath can be performed by directly sampling paths of the discretized harmonic modes and then propagating the system under the influence of random Gaussian field [37]. As such, the quantum dissipative dynamics can be conveniently simulated with the stochastic differential equation. Following the interpretation of Feynman, Stockburger and Grabert resolved the influence functional with Gaussian colored noises and derived a stochastic Liouville equation for the reduced density matrix [38–40]. Strunz, Yu and coworkers presented the non-Markovian quantum state diffusion method to describe the dynamics of the open system in terms of the stochastic Schrödinger's equation [41–46]. Alternatively, Breuer suggested the quantum jump approach and transferred the full non-Markovian reduced dynamics into Markovian random jump processes [47]. A stochastic description of a linear open quantum system was also developed by Calzetta and coworkers [48].

Our group put forward a stochastic Liouville equation for the dissipative dynamics of the system by decoupling the system-bath interaction in the equation of motion directly [49]. In this way the system-bath correlation is represented with the common random fields exerting on both the system and the bath. It is general and applicable for arbitrary types of bath and system-bath coupling. For the linear dissipation, it can be recast into the same form suggested by Stockburger and Grabert [50].

This review will focus on the stochastic description of dissipative systems. Special emphasis is placed on numerical simulations of dissipated two-level systems. Section 2 presents a detailed derivation of the stochastic Liouville equation via a stochastic decoupling of the quantum dissipative interaction. Both non-Hermitian and Hermitian schemes are derived and their numerical performance is discussed. Section 3 gives numerical examples for dissipated two-level systems with the stochas-

tic schemes. In Section 4 we demonstrate that the exact master equation for analytically solvable models can be conveniently worked out, starting from the stochastic equation. For general systems with a decomposable bath response function we show that the hierarchical approach can be achieved and is efficient at intermediate to high temperatures in Section 5. For dynamics at zero temperature or low temperatures, we suggest the hybrid stochastic-hierarchical equation in Section 6. The last section gives a brief summary and discusses the remaining challenges.

2 Decoupling system-bath interaction

Because of the couplings between the system and the bath, one has to take into account of the influence of the heat bath in order to describe the dynamics of the system exactly. For the description of the dissipative dynamics, we start with the system-plus-model [34],

$$\hat{H} = \hat{H}_s + \hat{H}_b + f(\hat{s})g(\hat{b}), \tag{1}$$

where $\hat{H}_s$ and $\hat{H}_b$ specify the relevant system and the bath, respectively. The system operator $\hat{s}$ describes the coupling to the bath with an arbitrary function $g(\hat{b})$ of the bath operator $\hat{b}$. In quantum mechanics the general interaction is a sum of force-field terms $\sum_j f_j(\hat{s})g_j(\hat{b})$. To simplify the formalism, we first investigate the above factorized form and discuss the extension to multiple terms in Section 2.2. Eq. (1) is for general bath and system-bath coupling. It becomes the Caldeira–Leggett model if the bath consists of an infinite independent quantum harmonic oscillators with linear system-bath coupling, i.e., $g(\hat{b}) = \sum_j c_j \hat{x}_j$ and a proper counterterm is included in the system Hamiltonian $\hat{H}_s$ [35].

The dynamics of the whole system is determined by the density matrix $\rho(t)$ which satisfies the Liouville–von Neumann equation

$$\mathrm{i}\hbar \mathrm{d}\rho/\mathrm{d}t = [\hat{H}, \rho(t)], \tag{2}$$

with an initial condition $\rho(0)$ at $t = 0$. Because we are only interested in the dynamical behavior of the system, the reduced density matrix $\rho_s(t) = \mathrm{tr}_b[\rho(t)]$ contains sufficient information for the reduced dynamics. Therefore, it is desired that the influence of the bath should be incorporated without the explicit consideration of the bath. This could be done by stochastically decoupling the dissipation interaction.

2.1 Heuristic decoupling via stochastic fields

The propagation of the density matrix, in turn, the intrinsic dynamical feature of the system, is dictated by the time evolution operator $U(t) \equiv \exp(-i\hat{H}t/\hbar)$. The propagator can be split along the time axis with Suzuki–Trotter expansion [51]

$$U(t) = \prod_{j=1}^{N} U(\Delta t), \quad \Delta t = t/N, \tag{3}$$

where the propagator for a short time interval Δt is approximated as

$$U(\Delta t) \approx \mathrm{e}^{-\mathrm{i}\hat{H}_s\Delta t/\hbar}\mathrm{e}^{-\mathrm{i}\hat{H}_b\Delta t/\hbar}\mathrm{e}^{-\mathrm{i}f(\hat{s})g(\hat{b})\Delta t/\hbar}. \tag{4}$$

Here, the first two factors are due to the contributions of the system and the bath, respectively, whereas the last one originates from the system-bath coupling. Because the operators $f(\hat{s})$ and $g(\hat{b})$ commutate, one can invoke the Hubbard–Stratonovich transformation to decouple the last factor [49]

$$\mathrm{e}^{-\mathrm{i}\Delta t f(\hat{s})g(\hat{b})/\hbar} = \frac{\Delta t}{2\pi}\int \mathrm{d}\upsilon_{1,j}\mathrm{d}\upsilon_{2,j}\mathrm{e}^{-(\upsilon_{1,j}^2+\upsilon_{2,j}^2)\Delta t/2} \times \mathrm{e}^{\mathrm{i}\Delta t(\upsilon_{1,j}+\mathrm{i}\upsilon_{2,j})f(\hat{s})/\sqrt{2\hbar}-\Delta t(\upsilon_{1,j}-\mathrm{i}\upsilon_{2,j})g(\hat{b})/\sqrt{2\hbar}}. \tag{5}$$

As the decoupling procedure is applied to every time step, the time evolution operator $U(t)$ is thus expressed as

$$U(t) = \left(\frac{\Delta t}{2\pi}\right)^N \int_{-\infty}^{\infty} \mathrm{d}\upsilon_{1,1}\cdots\mathrm{d}\upsilon_{1,N}\mathrm{d}\upsilon_{2,1}\cdots\mathrm{d}\upsilon_{2,N} \times \prod_{j=1}^{N}\Big(\mathrm{e}^{-\mathrm{i}\hat{H}_s\Delta t/\hbar}\mathrm{e}^{-\mathrm{i}\hat{H}_b\Delta t/\hbar}\mathrm{e}^{(\upsilon_{1,j}^2+\upsilon_{2,j}^2)\Delta t/2} \times \mathrm{e}^{\mathrm{i}\Delta t(\upsilon_{1,j}+\mathrm{i}\upsilon_{2,j})f(\hat{s})/\sqrt{2\hbar}-\Delta t(\upsilon_{1,j}-\mathrm{i}\upsilon_{2,j})g(\hat{b})/\sqrt{2\hbar}}\Big). \tag{6}$$

In the limit of $N \to \infty$, the integration becomes a path integral

$$U(t) = \int D[\upsilon_1]D[\upsilon_2]W[\upsilon_1,\upsilon_2]U_s[\upsilon_1,\upsilon_2]U_b[\upsilon_1,\upsilon_2], \tag{7}$$

where $\upsilon_1(t)$ and $\upsilon_2(t)$ now are two time-dependent external fields acting on the two subsystems and U_s and U_b are the propagators dictated by the "decoupled" system and the bath described respectively by the Hamiltonian $\tilde{H}_s(t) = H_s + \sqrt{\hbar}[\upsilon_1(t) + \mathrm{i}\upsilon_2(t)]f(\hat{s})/\sqrt{2}$ and $\tilde{H}_b(t) = H_b + \sqrt{\hbar}[\upsilon_2(t) + \mathrm{i}\upsilon_1(t)]g(\hat{b})/\sqrt{2}$. In Eq. (7), the weight functional $W[\upsilon_1,\upsilon_2] = \exp[-\int_0^t d\tau(\upsilon_{1,\tau}^2+\upsilon_{2,\tau}^2)/2]$ is the probability of the path. Due to the Gaussian functional form of the weight $W[\upsilon_1,\upsilon_2]$, $\upsilon_1(t)$ and $\upsilon_2(t)$ are two Gaussian white noises with mean $\mathcal{M}\langle\upsilon_j(t)\rangle = 0$ and correlation $\mathcal{M}\langle\upsilon_j(t)\upsilon_k(t')\rangle = \delta_{jk}\delta(t-t')$. Therefore, the exact evolution operator is the stochastic average of the combined propagator $U_s[\upsilon_1,\upsilon_2]U_b[\upsilon_1,\upsilon_2]$ with respect to two noises $\upsilon_1(t)$ and $\upsilon_2(t)$,

$$U(t) \equiv \mathcal{M}\langle U_s[\upsilon_1,\upsilon_2]U_b[\upsilon_1,\upsilon_2]\rangle, \tag{8}$$

where $\mathcal{M}$ denotes the stochastic averaging. Apparently, upon introducing common random fields, there is no direct interaction between the system and the bath. As

a consequence, the stochastic system and bath evolve "independently". Note that the exact propagator is the average of the product of the two stochastic propagators. The decoupling scheme essentially converts the quantum interaction to the stochastic correlation manifested in the average. In this sense the system and the bath are decoupled. Now, the evolution of the system and the bath is separate for a factorized initial density matrix $\rho(0)=\rho_s(0)\rho_b(0)$, that is,

$$\rho_s(t)=U_s[v_1,v_2]\rho_s(0)U_s^\dagger[v_3,v_4], \tag{9}$$

$$\rho_b(t)=U_b[v_1,v_2]\rho_b(0)U_b^\dagger[v_3,v_4], \tag{10}$$

where two more white noise fields $v_3(t)$ and $v_4(t)$ are introduced to decouple the dissipative interaction for the backward propagation. Then the exact density matrix is obtained when taking the stochastic average of a product of the system and the bath density operators, $\rho(t)=\mathcal{M}\langle\rho_s(t)\rho_b(t)\rangle$.

One could start from Eqs. (9) and (10) to derive the equations of motion for the stochastic densities $\rho_s(t)$ and $\rho_b(t)$. However, the results would be lengthy. To have a compact form, we define two complex-valued Wiener processes

$$w_{1,t}=\int_0^t \mathrm{d}t'[v_1(t')+v_3(t')+\mathrm{i}v_2(t')-\mathrm{i}v_4(t')]/\sqrt{2},$$

$$w_{2,t}=\int_0^t \mathrm{d}t'[v_2(t')+v_4(t')+\mathrm{i}v_1(t')-\mathrm{i}v_3(t')]/\sqrt{2},$$

which have the properties

$$\mathcal{M}\langle \mathrm{d}w_{j,t}\rangle=\mathcal{M}\langle \mathrm{d}w_{j,t}\mathrm{d}w_{k,t}\rangle=0,$$
$$\mathcal{M}\langle \mathrm{d}w_{j,t}\mathrm{d}w_{k,t}^*\rangle=2\delta_{jk}\mathrm{d}t. \tag{11}$$

The equations of motion for $\rho_s(t)$ and $\rho_b(t)$ now become

$$\mathrm{i}\hbar\mathrm{d}\rho_s=[H_s,\rho_s(t)]\mathrm{d}t+\sqrt{\hbar}/2[f(\hat{s}),\rho_s(t)]\mathrm{d}w_{1,t}+\mathrm{i}\sqrt{\hbar}/2\{f(\hat{s}),\rho_s(t)\}\mathrm{d}w_{2,t}^*, \tag{12}$$

$$\mathrm{i}\hbar\mathrm{d}\rho_b=[H_b,\rho_b(t)]\mathrm{d}t+\sqrt{\hbar}/2[g(\hat{b}),\rho_b(t)]\mathrm{d}w_{2,t}+\mathrm{i}\sqrt{\hbar}/2\{g(\hat{b}),\rho_b(t)\}\mathrm{d}w_{1,t}^*. \tag{13}$$

Here, both the stochastic differential equation and the stochastic integral are in Itô form.

2.2 Decoupling via Itô calculus

Alternatively, one may decouple the dissipative interaction via Itô calculus. For this purpose, we may introduce white noises as common forces exerting on the system and the bath, write down a general linear form of the stochastic differential equations with indeterminate coefficients for the independent evolution of the density matrices $\rho_{s/b}(t)$, require the stochastic average $\mathcal{M}\langle\rho_s(t)\rho_b(t)\rangle$ satisfying the quantum Liouville-von Neumann equation, and solve the indeterminate coefficients in the stochastic differential equations.

We have to recognize two key properties of Itô calculus. One is the differential equation of the product of two Itô processes X_t and Y_t

$$\mathrm{d}(X_tY_t)=X_t\mathrm{d}Y_t+(\mathrm{d}X_t)Y_t+(\mathrm{d}X_t)\mathrm{d}Y_t, \tag{14}$$

which is the differential form for the integration by parts in Itô calculus. The last term in Eq. (14) has to be included because $\mathrm{d}w_{j,t}$ is of the order $\sqrt{\mathrm{d}t}$. The other property is the nonanticipating rule

$$\mathcal{M}\langle X_t\mathrm{d}w_{j,t}\rangle=\mathcal{M}\langle X_t\mathrm{d}w_{j,t}\mathrm{d}w_{k,t}\rangle=0, \tag{15a}$$

$$\mathcal{M}\langle X_t\mathrm{d}w_{j,t}\mathrm{d}w_{k,t}^*\rangle=2\delta_{jk}\mathcal{M}\langle X_t\rangle\mathrm{d}t, \tag{15b}$$

which is analogous to Eq. (11). It holds because the Itô process X_t is independent of the noise increments $\mathrm{d}w_{j,t}$ and $\mathrm{d}w_{j,t}^*$.

To illustrate the procedure of the decoupling, we will use the general Hamiltonian for the dissipated system

$$\hat{H}=\hat{H}_s+\hat{H}_b+\sum_j^{N_I} f_j(\hat{s})g_j(\hat{b}), \tag{16}$$

where N_I is the number of interaction terms. Basing on the heuristic derivation, we propose the following ansatz for the stochastic differential equations of the two subsystems

$$\mathrm{i}\hbar\mathrm{d}\rho_s=[\hat{H}_s,\rho_s]\mathrm{d}t+\sqrt{\hbar}\sum_j^{N_I}[f_j(\hat{s}),\rho_s]s_{j,1}\mathrm{d}w_{j,1}+\mathrm{i}\sqrt{\hbar}\sum_j^{N_I}\{f_j(\hat{s}),\rho_s\}s_{j,2}\mathrm{d}w_{j,2}, \tag{17a}$$

$$\mathrm{i}\hbar\mathrm{d}\rho_b=[\hat{H}_b,\rho_b]\mathrm{d}t+\sqrt{\hbar}\sum_j^{N_I}[g_j(\hat{b}),\rho_b]b_{j,1}\mathrm{d}w_{j,3}+\mathrm{i}\sqrt{\hbar}\sum_j^{N_I}\{g_j(\hat{b}),\rho_b\}b_{j,2}\mathrm{d}w_{j,4}, \tag{17b}$$

where $s_{j,a}$ and $b_{j,a}$ are coefficients to be determined and the Wiener processes $w_{j,a}$ could be real or complex.

We readily find the differential equation for the density matrix $\rho(t)=\mathcal{M}\langle\rho_s(t)\rho_b(t)\rangle$,

$$\begin{aligned}\mathrm{i}\hbar\mathrm{d}\rho&=\mathcal{M}\langle\mathrm{i}\hbar(\mathrm{d}\rho_s)\rho_b+\mathrm{i}\hbar\rho_s d\rho_b+\mathrm{i}\hbar(\mathrm{d}\rho_s)\mathrm{d}\rho_b\rangle\\&=\mathcal{M}\langle[\hat{H}_s,\rho_s]\rho_b\mathrm{d}t+[\hat{H}_b,\rho_b]\rho_s\mathrm{d}t\\&\quad-\mathrm{i}\sum_{j,k}^{N_I}[f_j(\hat{s}),\rho_s][g_k(\hat{b}),\rho_b]s_{j,1}b_{k,1}\mathrm{d}w_{j,1}\mathrm{d}w_{k,3}\\&\quad+\sum_{j,k}^{N_I}[f_j(\hat{s}),\rho_s]\{g_k(\hat{b}),\rho_b\}s_{j,1}b_{k,2}\mathrm{d}w_{j,1}\mathrm{d}w_{k,4}\\&\quad+\sum_{j,k}^{N_I}\{f_j(\hat{s}),\rho_s\}[g_k(\hat{b}),\rho_b]s_{j,2}b_{k,1}\mathrm{d}w_{j,2}\mathrm{d}w_{k,3}\end{aligned}$$

$$+\mathrm{i}\sum_{j,k}^{N_I}\{f_j(\hat{s}),\rho_s\}\{g_k(\hat{b}),\rho_b\}s_{j,2}b_{k,2}\mathrm{d}w_{j,2}\mathrm{d}w_{k,4}\rangle. \tag{18}$$

When the following requirements are satisfied

$$\begin{aligned}
&s_{j,1}b_{k,1}\mathcal{M}\langle \mathrm{d}w_{j,1}\mathrm{d}w_{k,3}\rangle = 0,\\
&s_{j,1}b_{k,2}\mathcal{M}\langle \mathrm{d}w_{j,1}\mathrm{d}w_{k,4}\rangle = \delta_{jk}\mathrm{d}t/2,\\
&s_{j,2}b_{k,1}\mathcal{M}\langle \mathrm{d}w_{j,2}\mathrm{d}w_{k,3}\rangle = \delta_{jk}\mathrm{d}t/2,\\
&s_{j,2}b_{k,2}\mathcal{M}\langle \mathrm{d}w_{j,2}\mathrm{d}w_{k,4}\rangle = 0,
\end{aligned} \tag{19}$$

Eq. (18) will reproduce the Liouville–von Neumann equation. Although there are many possible choices for $s_{j,a}$ and $b_{k,a}$, we only consider the following simple settings,

$$\begin{aligned}
&\mathcal{M}\langle \mathrm{d}w_{j,a}\mathrm{d}w_{k,c}\rangle = 0, \quad \mathcal{M}\langle \mathrm{d}w_{j,a}\mathrm{d}w^*_{k,c}\rangle = \delta_{jk}\delta_{ac},\\
&w_{j,3} = w^*_{j,2}, \quad w_{j,4} = w^*_{j,1},
\end{aligned} \tag{20}$$

where $a, c = 1, 2$. When there is only one coupling term in Eq. (16), Eqs. (17a) and (17b) are nothing but Eqs. (12) and (13), respectively. Note that the so-obtained stochastic differential equation for the system, Eq. (17a) is non-Hermitian. We will discuss how to derive a Hermitian stochastic differential equation for the system using different settings of $s_{j,a}$, $b_{k,a}$ and $w_{j,a}$ in Section 2.4.

Once the decoupling scheme is chosen, one must proceed to establish the stochastic Liouville equation of the system by taking into account the influence of the bath. We will show that the impact of the bath can be characterized by the induced stochastic field.

2.3 Bath-induced stochastic field

Although the system and the bath are decoupled, they are still correlated because the real physical quantities are averages over the common stochastic fields that they are subject to. For instance, the reduced density matrix is obtained as $\tilde{\rho}_s(t) = \mathrm{tr}_b\mathcal{M}\langle\rho_s(t)\rho_b(t)\rangle = \mathcal{M}\langle\rho_s(t)\mathrm{tr}_b\rho_b(t)\rangle$. Once the trace of the bath is solved, the effect of the bath on the evolution of the system can be taken into account. This implies that the trace of the random bath includes the effect of the bath on the reduced dynamics. One may take the trace of Eq. (13) to find

$$\mathrm{tr}_b\rho_b(t) = \exp\left[\int_0^t \bar{g}(t')\mathrm{d}w^*_{1,t'}/\sqrt{\hbar}\right], \tag{21}$$

where $\bar{g}(t) = \mathrm{tr}_b\{\rho_b(t)g(\hat{b})\}/\mathrm{tr}_b\rho_b(t)$.

In performing the stochastic average to calculate the reduced density matrix, it is more convenient to include the contribution from the bath by absorbing the trace of $\rho_b(t)$ into the probability measure of the random fields. This can be achieved by applying the Girsanov transformation [52]. To illustrate the transformation clearly, we resort to the path integral form of the stochastic average,

$$\begin{aligned}
\tilde{\rho}_s(t) = &\int \mathcal{D}[w_1]\mathcal{D}[w_1^*]\mathcal{D}[w_2]\mathcal{D}[w_2^*]W[w_1,w_2]\\
&\times\rho_s[\mathrm{d}w_1,\mathrm{d}w_2^*;t]\exp\left[\int_0^t \mathrm{d}w^*_{1,\tau}\bar{g}(\tau)/\sqrt{\hbar}\right].
\end{aligned} \tag{22}$$

Here the notation $\rho_s[\mathrm{d}w_1,\mathrm{d}w_2^*;t]$ is used to refer to the functional dependence of the density matrix $\rho_s(t)$ on the stochastic processes. As the exponential factor formally assumes a Gaussian form, one may employ the Girsanov transformation, namely,

$$w_{1,t} = \tilde{w}_{1,t} + 2\int_0^t \mathrm{d}t'\bar{g}(t')/\sqrt{\hbar}, \tag{23}$$

to absorb the contribution from the bath. This transformation leaves $\bar{g}(t)$ invariant because $\rho_b(t)$, hence $\bar{g}(t)$, depends on only w_1^* and w_2, but not w_1 and w_2^*. As a result, Eq. (22) becomes

$$\begin{aligned}
\tilde{\rho}_s(t) = &\int \mathcal{D}[\tilde{w}_1]\mathcal{D}[\tilde{w}_1^*]\mathcal{D}[\tilde{w}_2]\mathcal{D}[\tilde{w}_2^*]W[w_1,w_2]\\
&\times\rho_s[\mathrm{d}\tilde{w}_1 + 2\bar{g}\mathrm{d}t/\sqrt{\hbar},\mathrm{d}\tilde{w}_2^*;t]\\
= &\mathcal{M}\langle\rho_s[\mathrm{d}\tilde{w}_1 + 2\bar{g}\mathrm{d}t/\sqrt{\hbar},\mathrm{d}\tilde{w}_2^*;t]\rangle.
\end{aligned} \tag{24}$$

This equation shows that the measure of the stochastic processes $w_{1,t}$ and $w_{2,t}$ keep unchanged while the differential equation for the stochastic density matrix of the system is transformed to

$$\begin{aligned}
\mathrm{i}\hbar\mathrm{d}\rho_s = &[H_s + \bar{g}(t)f(\hat{s}),\rho_s]\mathrm{d}t + \sqrt{\hbar}/2\,[f(\hat{s}),\rho_s]\,\mathrm{d}w_{1,t}\\
&+\mathrm{i}\sqrt{\hbar}/2\,\{f(\hat{s}),\rho_s\}\,\mathrm{d}w^*_{2,t}.
\end{aligned} \tag{25}$$

Now the reduced density matrix is yielded by directly taking the stochastic average of $\rho_s(t)$ over the noises $w_{1,t}$ and $w_{2,t}$, that is, $\tilde{\rho}_s(t) = \mathcal{M}\langle\rho_s(t)\rangle$. In words, once the function $\bar{g}(t)$ is known, the reduced dynamics can be solved without the need of explicit treatment of the bath at all. The role that $\bar{g}(t)$ plays becomes obvious: like the influence functional in the path integral treatment [53], it is the bath-induced field fully representing the influence of the environment.

So far the stochastic formalism is general, which is suitable for arbitrary baths. Using this formalism as a working procedure, we will focus on the Caldeira-Leggett model. In this case, because the dynamics of the bath is analytically solvable, one readily obtains the bath-induced stochastic field $\bar{g}(t)$. As usual, we assume that the bath starts from a thermal equilibrium state of noninteracting harmonic oscillators $\rho_b(0) = \exp(-\beta\hat{H}_b)/\mathrm{tr}_b[\exp(-\beta\hat{H}_b)]$, where $\beta = 1/(k_BT)$ is the inverse of the absolute temperature T scaled by the Boltzmann constant k_B. The trace for the stochastic

density matrix of the bath in Eq. (13) can be conveniently worked out in the interaction picture,

$$\rho_b(t) = U_0^{(b)}(t)U_+^{(b)}(t)\rho_b(0)U_-^{(b)}(t)U_0^{(b)\dagger}(t). \tag{26}$$

Here $U_0^{(b)}(t) = \exp(-\mathrm{i}\hat{H}_b t/\hbar)$ is the propagator of the free bath and $U_\pm^{(b)}(t)$ are the forward/backward propagators in the interaction picture satisfying the Itô differential equations

$$\mathrm{i}\hbar \mathrm{d}U_+^{(b)}(t) = \hat{g}(t)U_+^{(b)}(t)\mathrm{d}\chi_t^+, \tag{27a}$$

$$-\mathrm{i}\hbar \mathrm{d}U_-^{(b)}(t) = U_-^{(b)}(t)\hat{g}(t)\mathrm{d}\chi_t^-, \tag{27b}$$

where $\hat{g}(t) = U_0^{(b)\dagger}(t)g(\hat{b})U_0^{(b)}(t)$ is the interaction presentation of the operator $g(\hat{b})$, and $\chi_t^\pm$ are the Wiener processes involved in the forward/backward propagation,

$$\chi_t^+ = \sqrt{\hbar}/2(w_{2,t} + \mathrm{i}w_{1,t}^*),$$
$$\chi_t^- = \sqrt{\hbar}/2(w_{2,t} - \mathrm{i}w_{1,t}^*).$$

Due to the unitarity of $U_0^{(b)}(t)$ and the cyclic permutation invariance of the trace operation, the trace of the bath is expressed as

$$\mathrm{tr}_b[\rho_b(t)] = \mathrm{tr}_b\big[U_-^{(b)}(t)U_+^{(b)}(t)\rho_b(0)\big]. \tag{28}$$

Note that we are using factorized initial condition. Because harmonic oscillators of the bath are noninteracting, the propagators $U_0^{(b)}(t)$ and $U_\pm^{(b)}(t)$, and the trace of the density matrix $\rho_b(t)$ are products of that of all the individual oscillators. The standard way to work out the operator $\hat{g}(t)$ is the using of the operator algebra method [54]. Alternatively, it may be calculated by solving the equations of motion for the interaction representation for the bath coordinate operators $\hat{x}_j(t)$ and momentum operators $\hat{p}_j(t)$

$$\frac{\mathrm{d}}{\mathrm{d}t}\hat{x}_j(t) = \hat{p}_j(t)/m_j,$$
$$\frac{\mathrm{d}}{\mathrm{d}t}\hat{p}_j(t) = -m_j\omega_j^2\hat{x}_j(t). \tag{29}$$

Combining the initial condition $\hat{x}_j(0) = \hat{x}_j$ and $\hat{p}_j(0) = \hat{p}_j$, one straightforwardly solves these equations and obtains the result

$$\hat{g}(t) = \sum_j c_j[\hat{x}_j\cos(\omega_j t) + \hat{p}_j/(m_j\omega_j)\sin(\omega_j t)]. \tag{30}$$

Eq. (30) is actually a sum of two time-dependent operators. Consequently, one may resort to the Baker-Campbell–Hausdorff formula [55–59] to solve Eq. (27), yielding

$$U_+^{(b)}(t) = \exp\Big(-\mathrm{i}\int_0^t \mathrm{d}\chi_\tau^+\hat{g}(\tau) - \frac{1}{2}\int_0^t \mathrm{d}\chi_\tau^+\int_0^\tau d\chi_s^+[\hat{g}(\tau),\hat{g}(s)]\Big), \tag{31a}$$

$$U_-^{(b)}(t) = \exp\Big(+\mathrm{i}\int_0^t \mathrm{d}\chi_\tau^-\hat{g}(\tau) - \frac{1}{2}\int_0^t \mathrm{d}\chi_\tau^-\int_\tau^t \mathrm{d}\chi_s^-[\hat{g}(\tau),\hat{g}(s)]\Big). \tag{31b}$$

For linearly driven harmonic oscillators, the formula terminates at the second order because the commutator $[\hat{g}(\tau),\hat{g}(s)] = \mathrm{i}\hbar\sum_j c_j^2/(m_j\omega_j)\sin[\omega_j(\tau-s)]$ is a scalar function.

The product $U_-^{(b)}(t)U_+^{(b)}(t)$ can also be expressed as a single exponential function by using the Baker-Campbell–Hausdorff formula. Again, the first- and second-order terms yield the exact result for the linear bath,

$$\begin{aligned}U_-^{(b)}(t)U_+^{(b)}(t) = \exp\Big(&-\mathrm{i}\int_0^t \mathrm{d}\chi_\tau^+\hat{g}(\tau) + \mathrm{i}\int_0^t \mathrm{d}\chi_\tau^-\hat{g}(\tau)\\ &+\frac{1}{2}\int_0^t \mathrm{d}\chi_\tau^-\int_0^t \mathrm{d}\chi_s^+[\hat{g}(\tau),\hat{g}(s)]\\ &-\frac{1}{2}\int_0^t \mathrm{d}\chi_\tau^+\int_0^\tau \mathrm{d}\chi_s^+[\hat{g}(\tau),\hat{g}(s)]\\ &-\frac{1}{2}\int_0^t \mathrm{d}\chi_\tau^-\int_\tau^t \mathrm{d}\chi_s^-[\hat{g}(\tau),\hat{g}(s)]\Big).\end{aligned} \tag{32}$$

Calculating the quantum expectation and doing some rearrangements, we finally find the result for the trace of the bath,

$$\mathrm{tr}_b[\rho_b(t)] = \mathrm{e}^{\int_0^t \mathrm{d}w_{1,\tau}^*\int_0^\tau[\mathrm{d}w_{1,s}^*\alpha_r(\tau-s)+\mathrm{d}w_{2,s}\alpha_i(\tau-s)]}, \tag{33}$$

where $\alpha_r(t)$ and $\alpha_i(t)$ are the real and imaginary parts of the equilibrium correlation function $\alpha(t-s) = \mathrm{tr}_b[\hat{g}(t)\hat{g}(s)\rho_b(0)]$, respectively. For the linear dissipation model the correlation function becomes

$$\alpha(t) = \frac{1}{\pi}\int_0^\infty \mathrm{d}\omega J(\omega)\left[\coth\left(\frac{\beta\hbar\omega}{2}\right)\cos(\omega t) - \mathrm{i}\sin(\omega t)\right], \tag{34}$$

where $J(\omega)$ is the spectral density of the bath

$$J(\omega) = \frac{\pi}{2}\sum_j \frac{c_j^2}{m_j\omega_j}\delta(\omega-\omega_j). \tag{35}$$

A comparison between Eq. (21) and Eq. (33) yields the bath-induced field [49],

$$\bar{g}(t) = \sqrt{\hbar}\int_0^t \left[\mathrm{d}w_{1,t'}^*\alpha_r(t-t') + \mathrm{d}w_{2,t'}\alpha_i(t-t')\right]. \tag{36}$$

One observes that the correlation function of the bath serves as a memory kernel in the bath-induced field.

The stochastic description is flexible because it is allowed to make a free combination of the white noise and the bath-induced stochastic field or noise $\bar{g}(t)$ expressed

by Eq. (25). Doing so, one may obtain different composite Gaussian noises that affects the feasibility and efficiency of the numerical implementation. For instance, when the involved noises are rearranged such that

$$\xi_{1,t} = \frac{\bar{g}(t)}{\sqrt{\hbar}} + \frac{1}{2}\frac{\mathrm{d}w_{1,t}}{\mathrm{d}t},$$
$$\xi_{2,t} = \frac{1}{2}\frac{\mathrm{d}w^*_{2,t}}{\mathrm{d}t},$$

one recovers the stochastic formulation put forward by Stockburger and Grabert [50],

$$i\hbar\dot{\hat{\rho}}_s = [\hat{H}_s, \rho_s(t)] + \sqrt{\hbar}\,[f(\hat{s}), \rho_s(t)]\,\xi_{1,t} + \mathrm{i}\sqrt{\hbar}\,\{f(\hat{s}), \rho_s(t)\}\,\xi_{2,t}. \tag{37}$$

Here, the stochastic variables $\xi_{1(2),t}$ are Gaussian colored noises with means and correlations

$$\begin{aligned}
&\mathcal{M}\langle\xi_{1,t}\rangle = \mathcal{M}\langle\xi_{1,t}\rangle = 0,\\
&\mathcal{M}\langle\xi_{1,t}\xi_{1,\tau}\rangle = \alpha_r(t-\tau),\\
&\mathcal{M}\langle\xi_{1,t}\xi_{2,\tau}\rangle = \Theta(t-\tau)\alpha_i(t-\tau),\\
&\mathcal{M}\langle\xi_{2,t}\xi_{2,\tau}\rangle = 0,
\end{aligned} \tag{38}$$

where δ is the Dirac δ-function and Θ is the Heaviside step function

$$\Theta(x) = \begin{cases} 0, & \text{if } x \le 0,\\ 1, & \text{if } x > 0. \end{cases} \tag{39}$$

2.4 Hermitian stochastic Liouville equation

In general there are two major factors that influence the numerical performance of the stochastic formulation. One factor is the number of involved noises and the other is the intrinsic property of the stochastic differential equation, which may cause a stochastic realization dramatically different from the exact average. For the former, because the stochastic averaging over a larger number of noises corresponds to higher dimensional functional integration, the convergence normally becomes slower. Note that, although in our case there are four real noises in Eqs. (25) and (37), one can simply choose $\xi_{1,t}$ as a real noise to reduce the total number of noises to three [39]. For the latter, the stochastic density matrices Eqs. (25) and (37) do not preserve norm-conserving, hermicity and positivity that the exact one must do. Generally speaking, the more properties the stochastic density matrix possesses like the exact one, the better numerical performance the stochastic method will have. It is expected that a Hermitian stochastic scheme could be more efficient in the numerical convergence. We then suggest the following stochastic scheme [60]

$$\mathrm{i}\hbar\mathrm{d}\hat{\rho}_s = [\hat{H}_s, \hat{\rho}_s]\mathrm{d}t + \sqrt{\hbar/2}[f(\hat{s}), \hat{\rho}_s]\mathrm{d}\mu_2 + \mathrm{i}\sqrt{\hbar/2}\{f(\hat{s}), \hat{\rho}_s\}\mathrm{d}\mu_1, \tag{40}$$

$$\mathrm{i}\hbar d\hat{\rho}_b = [\hat{H}_b, \hat{\rho}_b]\mathrm{d}t + \sqrt{\hbar/2}[g(\hat{b}), \hat{\rho}_b](\mathrm{d}\mu_1 + \mathrm{i}\mathrm{d}\mu_4) + \mathrm{i}\sqrt{\hbar/2}\{g(\hat{b}), \hat{\rho}_b\}(\mathrm{d}\mu_2 + \mathrm{i}\mathrm{d}\mu_3). \tag{41}$$

This equation corresponds to the stochastic decoupling with Eq. (17) upon using the following parameters

$$\begin{aligned}
&s_{1,1} = s_{1,2} = b_{1,1} = b_{1,2} = 1/\sqrt{2},\\
&w_{1,1} = \mu_2, \quad w_{1,2} = \mu_1,\\
&w_{2,1} = \mu_1 + \mathrm{i}\mu_4, \quad w_{2,2} = \mu_2 + \mathrm{i}\mu_3,
\end{aligned} \tag{42}$$

for solving Eq. (19).

Knowing the trace of $\hat{\rho}_b(t)$, one can solve the reduced dynamics by taking a two-step stochastic average $\tilde{\rho}_s(t) = \mathcal{M}_{\mu_1,\mu_2}\langle\hat{\rho}_s(t)\mathcal{M}_{\mu_3,\mu_4}\{\mathrm{tr}_b[\hat{\rho}_b(t)]\}\rangle$ as the evolution of the random system does not depend on the noises $\mu_3(t)$ and $\mu_4(t)$.

Because Eq. (41) assumes the same form as Eq. (13), the trace of the random density matrix $\hat{\rho}_b(t)$ is given by Eq. (33) with the replacement $\mathrm{d}w^*_1 \to \sqrt{2}(\mathrm{d}\mu_1 + \mathrm{i}\mathrm{d}\mu_3)$ and $\mathrm{d}w_2 \to \sqrt{2}(\mathrm{d}\mu_2 + \mathrm{i}\mathrm{d}\mu_4)$. The stochastic average with respect to the Wiener processes $\mu_3(t)$ and $\mu_4(t)$ is a Gaussian type functional integration, which can be solved analytically

$$\mathcal{M}_{\mu_3,\mu_4}\langle\mathrm{tr}[\hat{\rho}_b(t)]\rangle = \exp\Big\{\frac{1}{2}\sum_{a,b=1}^{2}\int_0^t \mathrm{d}\mu_{a,\tau}\int_0^t \mathrm{d}\mu_{b,s} \times \Big[\delta_{ab}\delta(\tau - s) - \frac{1}{2}G_{ab}(\tau - s)\Big]\Big\}, \tag{43}$$

where $G(t-s)$ is the Green function of the correlation matrix function $\Gamma(t-\tau)$

$$\Gamma(t) = \begin{pmatrix} c\delta(t) + \alpha_r(t) & \Theta(t)\alpha_i(t)\\ \Theta(-t)\alpha_i(-t) & c\delta(t)\end{pmatrix}, \tag{44}$$

with $c = 1/2$. The right hand side of Eq. (43) assumes a Gaussian functional form and serves as a multiplicative factor in the stochastic average of the random density matrix $\hat{\rho}_s(t)$. Consequently, it can be combined with the Wiener measure of the noises $\mu_1(t)$ and $\mu_2(t)$ in taking the stochastic average

$$\begin{aligned}
\tilde{\rho}_s(t) &= \int \mathcal{D}[\mu_1]\mathcal{D}[\mu_2]W[\mu_1,\mu_2] \times \hat{\rho}_s(t)\mathcal{M}_{\mu_3,\mu_4}\langle\mathrm{tr}[\hat{\rho}_b(t)]\rangle\\
&= \int \mathcal{D}[\mu_1]\mathcal{D}[\mu_2]\mathrm{e}^{-\frac{1}{4}\sum_{a,b=1}^{2}\int_0^t \mathrm{d}\mu_{a,\tau}\int_0^t \mathrm{d}\mu_{b,s}G_{ab}(\tau-s)}\hat{\rho}_s(t).
\end{aligned}$$

The exponential part is still of the Gaussian functional form and can be treated as the measure of new Gaussian noises. With the change of variables according to $\mu_{1,t} = \sqrt{2}\int_0^t \mathrm{d}\tau\xi_{1,\tau}$ and $\mu_{2,t} = \sqrt{2}\int_0^t \mathrm{d}\tau\xi_{2,\tau}$, the stochastic differential equation for the density matrix assumes the same form as Eq. (37) but with noise averages $\mathcal{M}[\xi_{a,t}] = 0$ and new correlation functions $\mathcal{M}[\xi_{a,t}\xi_{b,\tau}] = \Gamma_{ab}(t-\tau)$.

It is expected that the Hermitian formulation will show a better numerical efficiency because of the hermicity and the smaller number of noises involved. Moreover, it was proven that the constant c in Eq. (44) can be arbitrarily chosen as long as the correlation function is semi-positive definite [60]. Simulations with the minimum allowed c value will further improve the numerical performance.

3 Stochastic simulations of spin-boson model

Given the initial state of the system and the bath-induced stochastic field $\bar{g}(t)$, one can solve Eq. (25) or Eq. (37) to obtain a stochastic trajectory. In general, the system of interest is a small one and the calculation of a single stochastic trajectory can be easily carried out. Note, however, that in the stochastic scheme the system is subject to the stochastic field characterizing the environment effect and one has to calculate many random trajectories to reach the convergent statistical expectation of the reduced density matrix. Roughly speaking, it is the statistics that makes the problem difficult.

We use the dissipated two-level system to demonstrate the implementation and efficiency of methods based on the stochastic formalism. Why are we interested in the spin-boson model? Well, as the two-level system is the simplest model characterizing quantum coherence, the unique feature in the microscopic world, the spin-boson model would be the most basic defining the fundamental paradigms of quantum dissipation. Moreover, the dynamics of the spin-boson model has been a challenge for many years. It is appropriate to cite Weiss here, "Despite its apparent simplicity, the spin-boson model cannot be solved exactly by any known method (apart from some limited regimes of the parameter space). Not only is the spin-boson model nontrivial mathematically, it is also nontrivial physically." [34]

We now consider the numerical simulation of the stochastic density matrix of the spin-boson model. To this end, we discretize the time using a uniform grid $\{0, t_1, \cdots, t_k, \cdots\}, (t_k = k\Delta t)$ with a fixed step-size Δt. Then, utilizing the conventional splitting operator technique, we obtain the iteration relation for propagation

$$\rho(t_{k+1}) = \mathrm{e}^{-\mathrm{i}\hat{H}_s\Delta t/\hbar - \mathrm{i}f(\hat{s})[\bar{g}_k\Delta t/\hbar + \sqrt{\hbar}/2(\Delta w_{1,k} + \mathrm{i}\Delta w^*_{2,k})]} \times \rho(t_k)\mathrm{e}^{\mathrm{i}\hat{H}_s\Delta t/\hbar + \mathrm{i}f(\hat{s})[\bar{g}_k\Delta t/\hbar + \sqrt{\hbar}/2(\Delta w_{1,k} - \mathrm{i}\Delta w^*_{2,k})]}. \quad (45)$$

The quantity $\Delta w_{a,k}$ is the change of the Wiener path in the time interval $[t_k, t_{k+1}]$. In the fixed step-size stochastic integration, one can simply put $\Delta w_{a,k} = \sqrt{\Delta t}(B_{a,1,k} + \mathrm{i}B_{a,2,k})$ with $B_{a,j,k}$ being independent standard normal random numbers. The vector $\bar{g}_k$ is the discretized version for the bath-induced random field. Note that a direct summation

$$\bar{g}_k = \sqrt{\hbar}\sum_{j=0}^{k-1}\left[\alpha_r((k-j)\Delta t)\Delta w_{2,k} + \alpha_i((k-j)\Delta t)\Delta w^*_{1,k}\right]$$

takes $O(N^2)$ multiplication and addition operations for N-step propagation which becomes expensive for the long time dynamics. Fortunately, it is a convolution integral and can be generated with an $O(N\log N)$ algorithm by using the fast Fourier transform [61].

One may generate the Gaussian colored noises with circulant embedding of the correlation Eq. (38) [62, 63]. We will exemplify the generation of a stochastic field ζ_t with mean $\mathcal{M}[\zeta_t] = 0$ and correlation $\mathcal{M}[\zeta_t\zeta_s] = \alpha_r(t-s)$. Upon discretization, one may build a $2N\times 2N$ circulant matrix embedding the correlation matrix

$$C_{jk} = \begin{cases} \alpha_r(|j-k|\Delta t), & \text{if } |j-k| < N \\ \alpha_r(|2(N-1)-|j-k||\Delta t), & \text{if } |j-k| \geq N \end{cases}.$$

The two principal submatrices with the first and the last N columns and rows are the original covariance matrix. The circulant matrix is diagonalized by the discrete Fourier transform $F^\dagger CF = \Lambda$, where Λ is the diagonal matrix taking the eigenvalues of the circulant matrix and F is the $2N\times 2N$ discrete Fourier transform matrix. If all the eigenvalues are non-negative, one can form a $2N$-dimensional complex vector with standard Gaussian random numbers, multiply it with $\Lambda^{1/2}$, and carry out the discrete Fourier transform to obtain two real random vectors x and y, i.e., $x + \mathrm{i}y = F\Lambda^{1/2}z$. Now x and y are uncorrelated but have identical correlation matrix C. Thus their first half and second half are four colored noises with zero mean and autocorrelation function $\alpha_r(t)$. This procedure can be extended to generate multiple correlated Gaussian random fields and the interested readers can refer to Refs. [64] and [65] for further details.

To show how the stochastic formulation works, we take the quantum nondemolition measurement of the two-level system as the first numerical example. Specifically, $\hat{H}_s = \frac{1}{2}\sigma_z$, $f(\hat{s}) = \sigma_z$, and $\alpha(t) = \exp(\mathrm{i}t - 2|t|)/2$ are adopted with an initial condition $\tilde{\rho}_s(0) = 0.5I + 0.5\sigma_x + 0.6\sigma_y$. In this case the system Hamiltonian $\hat{H}_s$ commutates with the coupling operator $f(\hat{s})$ and there is no energy exchanging between the system and the bath [49, 66–68]. Accordingly, the diagonal elements in the eigen-energy representation do not change with time but the off-diagonal matrix elements are damped to zero, which is pure dephasing caused by the bath. The model is exactly solvable and the master equation reads

$$\mathrm{i}\hbar\dot{\tilde{\rho}} = [\hat{H}_s, \tilde{\rho}] - \mathrm{i}C_r(t)[f(\hat{s}), [f(\hat{s}), \tilde{\rho}]] + C_i(t)[f(\hat{s})^2, \tilde{\rho}],$$

where $C_{r/i} = \int_0^t \mathrm{d}\tau\alpha_{r/i}(t-\tau)$. The results of the stochastic simulations with noises generated from circulant embedding of Eq. (38) are depicted in Fig. 1. One clearly sees that the random average with 256 stochastic trajectories already produces the reduced density

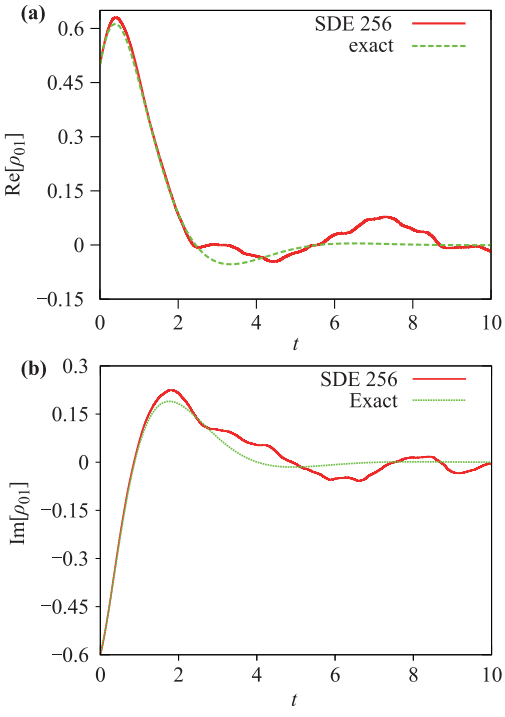

Fig. 1 The stochastic simulation for the coherence in a quantum nondemolition measurement. **(a)** The real and **(b)** the imaginary part of ρ_{01} with 256 stochastic trajectories are compared with the exact results.

matrix up to time $t = 2$ quite well for both the real and imaginary parts of the off-diagonal matrix element $\rho_{01}(t)$.

The second example is the spontaneous decay of a two-state atom at zero temperature. As its exact quantum master equation is known [31, 43, 47], the exact dynamics can be calculated numerically. It thus provides a good model for numerical tests of the stochastic scheme. The Hamiltonian for the dissipative system reads

$$\hat{H}_s = \frac{\hbar\Delta}{2}\sigma_z, \quad \hat{H}_b = \sum_j \hbar\omega_j b_k^\dagger b_k,$$

$$\hat{H}_{sb} = \sigma^-\hat{g}_1 + \sigma^+\hat{g}_2, \quad \hat{g}_1 = \hbar\sum_j c_j b_j^\dagger = \hat{g}_2^\dagger.$$

Here there are two coupling terms in the Hamiltonian, we will introduce two pairs of complex-valued Wiener processes and use parameters given in Eq. (20) for the stochastic Liouville equation Eq. (17). Following a similar procedure for Eqs. (26)–(22), we can solve the equation of motion for the bath to obtain the bath-induced random fields

$$\bar{g}_1(t) = \frac{\sqrt{\hbar}}{2}\int_0^t (\mathrm{d}w^*_{21,\tau} - \mathrm{i}\mathrm{d}w^*_{22,\tau})\alpha(t-\tau), \tag{46}$$

$$\bar{g}_2(t) = \frac{\sqrt{\hbar}}{2}\int_0^t (\mathrm{d}w^*_{11(4),\tau} + \mathrm{i}\mathrm{d}w^*_{21,\tau})\alpha^*(t-\tau), \tag{47}$$

with the response function of the bath $\alpha(t) = \sum_j |c_j|^2 \mathrm{e}^{\mathrm{i}\omega_j t}$. To simplify the notations we define

$$\mu_1 = (w_{11} - \mathrm{i}w_{12})/\sqrt{2}, \quad \mu_2 = (w_{21} + \mathrm{i}w_{22})/\sqrt{2},$$
$$\mu_3 = (w_{11} + \mathrm{i}w_{12})/\sqrt{2}, \quad \mu_4 = (w_{21} - \mathrm{i}w_{22})/\sqrt{2}.$$

Then the bath-induced fields are transformed to

$$\bar{g}_1(t) = \sqrt{\frac{\hbar}{2}}\int_0^t \mathrm{d}\mu^*_{2,\tau}\alpha(t-\tau),$$

$$\bar{g}_2(t) = \sqrt{\frac{\hbar}{2}}\int_0^t \mathrm{d}\mu^*_{1,\tau}\alpha^*(t-\tau).$$

As a consequence, the stochastic differential equation (17a) becomes

$$\mathrm{i}\hbar\mathrm{d}\hat{\rho}_s = [\hat{H}_s + \sigma^-\bar{g}_1(t) + \sigma^+\bar{g}_2(t), \hat{\rho}_s]\mathrm{d}t - \sqrt{\frac{\hbar}{2}}\hat{\rho}_s\sigma^-\mathrm{d}\mu_1$$
$$+\sqrt{\frac{\hbar}{2}}\sigma^+\hat{\rho}_s\mathrm{d}\mu_2 + \sqrt{\frac{\hbar}{2}}\sigma^-\hat{\rho}_s\mathrm{d}\mu_3 - \sqrt{\frac{\hbar}{2}}\hat{\rho}_s\sigma^+\mathrm{d}\mu_4. \tag{48}$$

Note that the bath-induced fields $\bar{g}_1(t)$ and $\bar{g}_2(t)$ are independent of the noises $\mu_3(t)$ and $\mu_4(t)$. We first take the average over $\mu_3(t)$ and $\mu_4(t)$ to obtain

$$\mathrm{i}\hbar\mathrm{d}\hat{\rho}_s = [\hat{H}_s + \sigma^-\bar{g}_1(t) + \sigma^+\bar{g}_2(t), \hat{\rho}_s]\mathrm{d}t$$
$$-\sqrt{\frac{\hbar}{2}}\hat{\rho}_s\sigma^-\mathrm{d}\mu_1 + \sqrt{\frac{\hbar}{2}}\sigma^+\hat{\rho}_s\mathrm{d}\mu_2. \tag{49}$$

Although $\hat{\rho}_s(t)$ in Eq. (49) is not the same as that in Eq. (48), their stochastic averages are identical. Eq. (49) assumes better numerical performance because it involves a smaller number of stochastic fields.

We generate the bath-induced random fields by the convolution method [61] and carry out the stochastic simulations with Eq. (49) using $\alpha(t) = \frac{\gamma}{2}\mathrm{e}^{-\gamma|t|+\mathrm{i}t}(\gamma = 0.1)$. The excited state population follows a non-exponential decay. As shown in Fig. 2, the results averaged with 2^{24} trajectories reproduce the damped oscillation very well and the maximum statistical error is less the 0.006 for all times.

In the third example we investigate the dynamics of the dissipated two-level system using the Hermitian scheme. The Hamiltonian and the coupling operator for the two-level system are

$$\hat{H}_s = \hbar\Delta\ \sigma_x/2, \quad f(\hat{s}) = \sigma_z/2, \tag{50}$$

where Δ is the tunneling matrix element. The spectral density is assumed to take an Ohmic form with the Debye regulation

$$J(\omega) = \eta\omega\omega_c^2/(\omega_c^2 + \omega^2), \tag{51}$$

where η is the dissipation strength and ω_c is the cut-off frequency. We will use a relatively large cut-off $\omega_c = 4\Delta$ with a moderate dissipation strength $\eta = 0.4$ for the

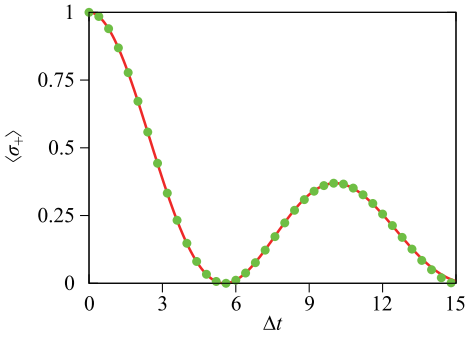

Fig. 2 Spontaneous decay of the excited state population of a two-state atom. Solid line: The exact results. Bullets: The stochastic simulations of Eq. (49) with 2^{24} realizations.

stochastic simulations. The corresponding correlation function can be expressed in terms of exponentials [69]

$$\alpha(t) = \frac{\eta\omega_c^2}{2}\left[\cot\left(\beta\hbar\omega_c/2\right) - \mathrm{i}\right]\mathrm{e}^{-\omega_c t} + \frac{2\eta\omega_c^2}{\hbar\beta}\sum_{k=1}^{\infty}\frac{\nu_k \mathrm{e}^{-\nu_k t}}{\nu_k^2 - \omega_c^2}, \tag{52}$$

where $\nu_k = 2\pi k/(\hbar\beta)$ is the kth Matsubara frequency of the bath.

The Hermitian scheme is integrated with the order 2 weak Runge–Kutta approximation [70]. The two correlated stochastic fields are generated with the circulant embedding approach. The number of time steps of the stochastic integration is 8192 with a step size of $0.001/\Delta$ and the number of trajectories is 40 million for all simulations at different temperatures. With these settings, it takes about 20 CPU hours with 16 Intel(R) Xeon(R) E5620 CPUs having a clock speed of 2.40 GHz.

Stochastic simulations with Eqs. (25) and (44) at temperatures of 0.001, 0.5, 1.0, 2.0, 3.0, 4.0 and 5.0 $\hbar\Delta/k_{\mathrm{B}}$ are performed. Numerical simulations based on the hierarchical approach outlined in Section 5 are carried out at temperatures 1.0–5.0 $\hbar\Delta/k_{\mathrm{B}}$ to serve as numerical benchmarks because this model is not exactly solvable.

The expectation $\sigma_z(t) = \langle\sigma_z\tilde{\rho}_s(t)\rangle$, the population difference between the left and right states is a key quantity for understanding the dynamics of the dissipated two-level system. The temperature dependence of the evolution of the population difference is depicted in Fig. 3. The dominant feature is the decrease of coherence at higher temperatures. Further calculations show that the population difference decrease monotonically when temperature is higher than 6 $\hbar\Delta/k_{\mathrm{B}}$. Another interesting observation is that the line for the positions of the minimum is not a straight line perpendicular to x-axis. This fact is the reflection of the mechanism for the temperature-dependent dephasing [71].

Figure 3(b) displays the deviations from the numerically exact results simulated with hierarchical approach.

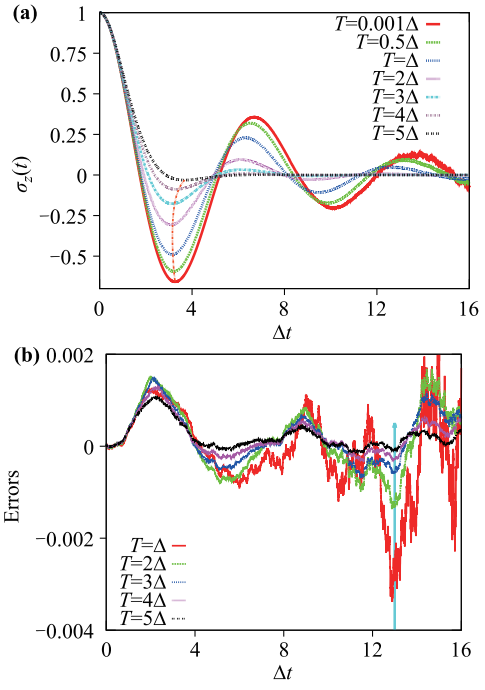

Fig. 3 **(a)** The temperature dependence of the time evolution for the population difference between the left and the right states. The line connecting the minimum of each curve is also shown. **(b)** The deviations of the stochastic simulations from the numerically exact hierarchical results. The errors are defined as $(\langle\sigma_z\rangle_{SDE} - \langle\sigma_z\rangle_{HE})/(1+|\langle\sigma_z\rangle_{HE}|)$ with $\langle\sigma_z\rangle_{SDE}$ being the results from the stochastic simulation and $\langle\sigma_z\rangle_{HE}$ that from the hierarchical approach. The temperature corresponding to the curves increases from the bottom to the top at the intersections with the connecting curve in (a) and the indicated arrow in (b).

One finds that the maximum errors are less than 0.004 up to the time $t = 16/\Delta$. If the results from the stochastic simulation are plotted on top of the hierarchical ones, the differences cannot be recognized with naked eye. Thus the non-Markovian non-perturbative stochastic master equation in Eq. (38) produces reliable results. The other main feature is that bigger errors occur at lower temperatures, as already noticed in the Monte-Carlo simulations.

Define the trace distance D between two quantum states $\rho_{1,2}$ [72]

$$D(\rho_1, \rho_2) = \frac{1}{2}\mathrm{tr}\sqrt{(\rho_1^\dagger - \rho_2^\dagger)(\rho_1 - \rho_2)}, \tag{53}$$

which is a natural metric on the state space based on the Schatten p-norm with $p = 1$ [73]. It satisfies $0 \le D \le 1$ and is invariant under unitary transformation, non-increasing for completely positive and trace-preserving quantum maps. Therefore, the trace distance is often interpreted as a measure for the distinguishability of quantum states. The quantity D is always decreas-

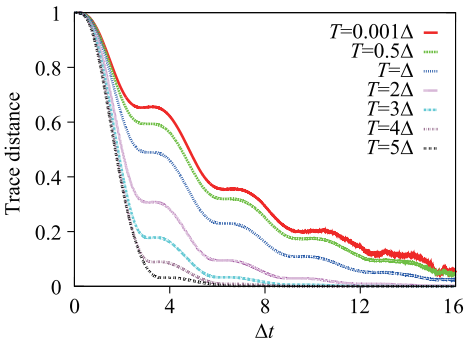

Fig. 4 The trace distance between the left and right states at different temperatures.

ing with time for Markovian propagation but sometimes increasing for non-Markovian processes. Breuer, Laine and Piilo suggested a measure for the non-Markovianity based on the increase of D [74]. Interested readers may refer to Ref. [75] for a recent review on the characterization and quantification of the non-Markovianity.

Note that the parity symmetry is preserved in the exact reduced dynamics of the model. The symmetry implies that the condition $\rho_2(t) = \sigma_x\rho_1(t)\sigma_x$ holds for any time if it is satisfied at the initial time for two quantum states $\rho_1(t)$ and $\rho_2(t)$. The parity symmetry allows us to explore the non-Markovianity of the model by calculating the trace distance between a quantum state and its symmetry image. Fig. 4 depicts the changes of the trace distance between the left state and its symmetry image (the right state) at different temperatures. It clearly depicts the trend that the trace distance approaches zero at long times. For all the simulated temperatures there exist time ranges with increasing distance, which is a clear sign of non-Markovianity. However, the increase becomes weaker at higher temperatures, which agrees with the intuition that the non-Markovianity becomes weaker as the temperature goes higher. We have also carried out the propagation of quantum trajectories starting from the right state to check the reliability of the symmetry based method. The differences between the two sets of results are always less than 5% regardless of time and temperature.

4 From stochastic to deterministic: Master equation

The direct application of the stochastic differential equation is only suitable for weak to intermediate dissipation. By contrast, deterministic methods are far more efficient to study moderate to strong dissipation. Unfortunately, exact deterministic method is not available for general systems and thus accurate approximations are required for the study of quantum dissipative dynamics. In developing approximations, analytically solvable models will be appreciated because they not only provide insightful understanding of quantum dissipation but also serve as benchmarks.

The stochastic scheme outlined in previous sections is useful to derive deterministic equations for certain dissipative systems. To this end, one should first take the stochastic average of Eq. (25) to obtain the deterministic equation of motion for the reduced density matrix,

$$\mathrm{i}\hbar\mathrm{d}\tilde{\rho}_s/\mathrm{d}t = [H_s, \tilde{\rho}_s(t)] + [f(\hat{s}), \mathcal{M}\langle\bar{g}(t)\rho_s(t)\rangle]. \tag{54}$$

In the above derivation the nonanticipating property Eq. (15) is used. Unfortunately, Eq. (54) is not in closed form because of the correlation between the stochastic density matrix $\rho_s(t)$ and the random field $\bar{g}(t)$. To work out a master equation one has to express the statistical average $\mathcal{M}\langle\bar{g}(t)\rho_s(t)\rangle$ explicitly in terms of the reduced density matrix and other known operators of the system. It is a challenging task to derive a deterministic method from a stochastic one for arbitrary noise [12, 76–78].

For the Caldeira–Leggett model, the stochastic average $\mathcal{M}\langle\bar{g}(t)\rho_s(t)\rangle$ in Eq. (54) can be formally expressed as follows by recognizing the expression of the bath-induced field

$$\mathcal{M}\langle\bar{g}(t)\rho_s(t)\rangle = \mathcal{M}\langle\hat{O}_R(t)\rangle + \mathcal{M}\langle\hat{O}_I(t)\rangle, \tag{55}$$

$$\hat{O}_{R(I)}(t) = \int_0^t \mathrm{d}t'\alpha_{r(i)}(t-t')\rho_{s,1(2)}(t,t'), \tag{56}$$

where $\rho_{s,1}(t,t') = \sqrt{\hbar}\,[\upsilon_1(t') - \mathrm{i}\upsilon_4(t')]\,\rho_s(t)$ and $\rho_{s,2}(t,t') = \sqrt{\hbar}\,[\upsilon_2(t') + \mathrm{i}\upsilon_3(t')]\,\rho_s(t)$. Here the real Gaussian white noises υ_j are connected to the Wiener processes $w_{1/2}$ through the relations $w_{1,t} = \int_0^t \mathrm{d}s[\upsilon_1(s) + \mathrm{i}\upsilon_4(s)]$ and $w_{2,t} = \int_0^t \mathrm{d}s[\upsilon_2(s) + \mathrm{i}\upsilon_3(s)]$. To obtain the expressions of $\mathcal{M}\langle\rho_{s,1(2)}(t,t')\rangle$ we resort to the Furutsu-Novikov theorem [79], that is,

$$\mathcal{M}\langle\upsilon(t')F[\upsilon]\rangle = \mathcal{M}\left\langle\frac{\delta F[\upsilon]}{\delta\upsilon(t')}\right\rangle \tag{57}$$

for a white noise υ and an arbitrary functional $F[\upsilon]$. Thanks to this theorem we are allowed to express the random average $\mathcal{M}\langle\rho_{s,1(2)}(t,t')\rangle$ in terms of functional derivatives

$$\begin{aligned}\mathcal{M}\left\langle\rho_{s,1}(t,t')\right\rangle &= \sqrt{\hbar}\mathcal{M}\left\langle\frac{\delta\rho_s(t)}{\delta\upsilon_1(t')} - \mathrm{i}\frac{\delta\rho_s(t)}{\delta\upsilon_4(t')}\right\rangle \\ &\equiv \hat{O}_{s,1}(t,t'),\end{aligned} \tag{58}$$

$$\begin{aligned}\mathcal{M}\left\langle\rho_{s,2}(t,t')\right\rangle &= \sqrt{\hbar}\mathcal{M}\left\langle\frac{\delta\rho_s(t)}{\delta\upsilon_2(t')} + \mathrm{i}\frac{\delta\rho_s(t)}{\delta\upsilon_3(t')}\right\rangle \\ &\equiv \hat{O}_{s,2}(t,t').\end{aligned} \tag{59}$$

Also by applying the Furutsu–Novikov theorem and recognizing the formal solution of $\rho_s(t)$, we find the results for the functional derivatives with another type of noise combination

$$\mathcal{M}\Big\{\frac{\delta\rho_s(t)}{\delta\upsilon_1(t')}+\mathrm{i}\frac{\delta\rho_s(t)}{\delta\upsilon_4(t')}\Big\}=\frac{2}{\sqrt{\hbar}}\int_{t'}^{t}\mathrm{d}s\alpha_r(s-t')\hat{O}_{s,1}(t,s),$$
$$\mathcal{M}\Big\{\frac{\delta\rho_s(t)}{\delta\upsilon_2(t')}-\mathrm{i}\frac{\delta\rho_s(t)}{\delta\upsilon_3(t')}\Big\}=\frac{2}{\sqrt{\hbar}}\int_{t'}^{t}\mathrm{d}s\alpha_i(s-t')\hat{O}_{s,2}(t,s). \tag{60}$$

To proceed, we invoke the formal solution of Eq. (25)

$$\rho_s(t)=U_+(t,0)\rho_s(0)U_-(0,t), \tag{61}$$

where $U_\pm(t,0)$ are the forward/backward propagator associated with the time-dependent stochastic Hamiltonian

$$\hat{H}_+(t)=\hat{H}_s+[\bar{g}(t)+\sqrt{\hbar}\eta_+(t)/2]f(\hat{s}), \tag{62}$$

and

$$\hat{H}_-(t)=\hat{H}_s+[\bar{g}(t)+\sqrt{\hbar}\eta_-(t)/2]f(\hat{s}), \tag{63}$$

respectively. Here $\eta_\pm(t)=\upsilon_{1,t}+\mathrm{i}\upsilon_{4,t}\pm\mathrm{i}\upsilon_{2,t}\pm\upsilon_{3,t}$ are the noises ascociated with the forward/backward propagation. By virtue of the stochastic propagator, one defines the Heisenberg operators $\hat{x}_\pm(t,t')=U_\pm(t,t')f(\hat{s})U_\pm(t',t)$. Then the operators $\hat{O}_{s,1(2)}(t,t')$ corresponding to the functional derivatives are re-expressed as

$$\hat{O}_{s,1}(t,t')=-\mathrm{i}\mathcal{M}\left\langle\hat{x}_+(t,t')\rho_s(t)-\rho_s(t)\hat{x}_-(t,t')\right\rangle,$$
$$\hat{O}_{s,2}(t,t')=\mathcal{M}\left\langle\hat{x}_+(t,t')\rho_s(t)+\rho_s(t)\hat{x}_-(t,t')\right\rangle. \tag{64}$$

Eq. (64) converts the task from solving $\mathcal{M}\{\bar{g}(t)\rho_s(t)\}$ to tackling $\hat{O}_{s,1(2)}(t,t')$ in terms of $\tilde{\rho}_s(t)$ and other known operators.

For arbitrary systems, deriving the master equation relies on whether the explicit expressions of dissipative operators $\hat{O}_{s,1(2)}(t,t')$ can be worked out or not. Unfortunately, it cannot be analytically solved for general systems. However, the master equation can be constructed when either the Hamiltonian of the system or the response function of the bath assumes special properties. Here we will present two examples, one with a special response function and the other with the harmonic oscillator Hamiltonian.

4.1 High-temperature approximations

First, we consider dissipative dynamics at the high-temperature limit. This is the classical regime, in which the bath response is more local in time. Thus one may resort to the Markovian approximation. We again consider the Caldeira–Leggett model, see Eq. (36). Note that in the bath-induced field the imaginary part of the memory function is independent of temperature, which is of a genuine quantum effect. At high temperatures (small β) we use the Taylor expansion of $\coth(\hbar\beta\omega)$ in the real part of the memory function to obtain the dominant contribution

$$\alpha_r(t)=\frac{2}{\pi}\int_0^\infty\mathrm{d}\omega\frac{J(\omega)}{\hbar\beta\omega}\cos(\omega t).$$

In the strict Ohmic dissipation $J(\omega)=\eta\omega$, the memory time of the bath response becomes zero, that is

$$\alpha_r(t)=\frac{2\eta}{\hbar\beta}\delta(t)$$

and

$$\alpha_i(t)=\eta\delta'(t).$$

It is a bit subtle to use the δ-functions because they are involved in the integral from 0 to t. In other words, only half of the distribution contributes to the integration. Without a rigorous proof we simply put down as

$$\int_0^t\mathrm{d}t'\delta(t')f(t')=\frac{1}{2}f(0),$$
$$\int_0^t\mathrm{d}t'\delta'(t')f(t')=-\frac{1}{2}f'(0).$$

These expressions can be substituted into Eq. (55) to obtain

$$\hat{O}_R(t)=\frac{\eta}{\sqrt{\hbar}\beta}\rho_{s,1}(t,t), \tag{65}$$

$$\hat{O}_I(t)=\frac{\eta}{2}\sqrt{\hbar}\ \frac{\partial}{\partial t'}\rho_{s,2}(t,t')\Big|_{t'=t}. \tag{66}$$

With the help of Eq. (25) we readily acquire

$$\mathcal{M}\langle\hat{O}_R(t)\rangle=-\frac{\mathrm{i}\eta}{\hbar\beta}[f(\hat{s}),\tilde{\rho}_s(t)], \tag{67}$$

$$\mathcal{M}\langle\hat{O}_I(t)\rangle=\frac{\mathrm{i}\eta}{2\hbar}\left\{[H_s,f(\hat{s})],\tilde{\rho}_s(t)\right\}. \tag{68}$$

Inserting into Eq. (55), we obtain the semiclassical master equation

$$\mathrm{i}\hbar\frac{\partial\tilde{\rho}_s}{\partial t}=[H_s,\tilde{\rho}_s]-\frac{\mathrm{i}\eta}{\hbar\beta}[f(\hat{s}),[f(\hat{s}),\tilde{\rho}_s]]+\frac{\mathrm{i}\eta}{2\hbar}[f(\hat{s}),\{[H_s,f(\hat{s})],\tilde{\rho}_s\}]. \tag{69}$$

For conventional systems $H_s=\hat{p}^2/(2M)+V_R(\hat{x})$ and $f(\hat{s})=\hat{x}$ there is $[H_s,f(\hat{s})]=-\mathrm{i}\hbar\hat{p}/M$. Note that the potential operator here includes the renormalization contribution $1/2M\tilde{w}^2\hat{x}^2$ with

$$\tilde{\omega}^2=\sum_j\frac{c_j^2}{m_j\omega_j^2}=\frac{2}{\pi}\int_0^\infty\mathrm{d}\omega\frac{J(\omega)}{\omega}. \tag{70}$$

Substituting into Eq. (69) leads to the well-known Caldeira–Leggett master equation

$$\mathrm{i}\hbar\frac{\partial\tilde{\rho}_s}{\partial t}=[H_s,\tilde{\rho}_s]-\frac{\mathrm{i}\eta}{\hbar\beta}[\hat{x},[\hat{x},\tilde{\rho}_s]]+\frac{\eta}{2M}[\hat{x},\{\hat{p},\tilde{\rho}_s\}]. \tag{71}$$

This equation has been frequently discussed from different perspectives in the literature, for instance, in

Ref. [80]. In this approximation the system follows the exact quantum dynamics while the environment is rather "classical" and Markovian as it is assumed to be at high temperatures. At low temperatures, the non-Markovian effect cannot be neglected and rigorous methods are required [40].

4.2 Master equation for dissipative harmonic oscillators

We consider a dissipative quantum harmonic oscillator as the second example. The dissipative harmonic oscillator is one among the few exactly solvable model for theoretical analysis and has been extensively studied in the literature [45, 48, 81–101]. Here we will follow Ref. [101] to present a brief derivation in a straightforward and elementary way through the stochastic decoupling approach.

Suppose the renormalized frequency of the quantum harmonic oscillator is ω when the contribution due to Eq. (70) is accounted. For such a linear system, the stochastic propagators $U_{\pm}(t,0)$ can be solved by using Eqs. (27)–(31) and the stochastic Heisenberg operators $\hat{x}_{\pm}(t,t')$ in Eq. (64) can be calculated correspondingly

$$\hat{x}_{\pm}(t,t') = \cos\omega(t-t')\hat{x} - \frac{\sin\omega(t-t')}{M\omega}\hat{p} - \frac{1}{M\omega}\int_{t'}^{t} \mathrm{d}t_1 \sin\omega(t_1-t')\left[\bar{g}(t_1) + \frac{\sqrt{\hbar}}{2}\eta_{\pm}(t_1)\right].$$

Inserting into Eq. (64) and carrying out the involved stochastic averaging, we obtain the following integral equations for the operators $\hat{O}_{s,1}$ and $\hat{O}_{s,2}$

$$\begin{aligned}\hat{O}_{s,1}(t,t') = &-\mathrm{i}\cos\omega(t-t')\left[\hat{x},\tilde{\rho}_s(t)\right] + \frac{\mathrm{i}}{M\omega}\sin\omega(t-t')\left[\hat{p},\tilde{\rho}_s(t)\right] \\ &+ \frac{2}{M\omega}\int_{t'}^{t}\mathrm{d}t_1\int_{t_1}^{t}\mathrm{d}t_2\sin\omega(t_1-t') \\ &\times\ \alpha_i(t_1-t_2)\hat{O}_{s,1}(t,t_2), \qquad (72)\\ \hat{O}_{s,2}(t,t') = &\cos\omega(t-t')\left\{\hat{x},\tilde{\rho}_s(t)\right\} - \frac{\sin\omega(t-t')}{M\omega}\left\{\hat{p},\tilde{\rho}_s(t)\right\} \\ &- \frac{2}{M\omega}\int_{t'}^{t}\mathrm{d}t_1\int_{0}^{t}\mathrm{d}t_2\sin\omega(t_1-t') \\ &\times\ \alpha_r(t_1-t_2)\hat{O}_{s,1}(t,t_2) \\ &- \frac{2}{M\omega}\int_{t'}^{t}\mathrm{d}t_1\int_{0}^{t_1}\mathrm{d}t_2\sin\omega(t_1-t') \\ &\times\ \alpha_i(t_1-t_2)\hat{O}_{s,2}(t,t_2). \qquad (73)\end{aligned}$$

Here, Eq. (60) is used to obtain these equations.

The linear integral equation Eq. (72) for $\hat{O}_{s,1}$ does not depend on $\hat{O}_{s,2}$ and can be solved at first. Taking into account the inhomogeneous term, a reasonable guess for the solution is

$$\hat{O}_{s,1}(t,t') = x_{11}(t,t')\left[\hat{p},\tilde{\rho}_s(t)\right] + x_{12}(t,t')\left[\hat{x},\tilde{\rho}_s(t)\right], \qquad (74)$$

which can be verified by iteration. With the same reasoning, the expression of $\hat{O}_{s,2}(t,t')$ possesses the following form

$$\begin{aligned}\hat{O}_{s,2}(t,t') = &\, x_{21}(t,t')\left\{\hat{x},\tilde{\rho}_s(t)\right\} + x_{22}(t,t')\left\{\hat{p},\tilde{\rho}_s(t)\right\} \\ &+ x_{23}(t,t')\left[\hat{p},\tilde{\rho}_s(t)\right] + x_{24}(t,t')\left[\hat{x},\tilde{\rho}_s(t)\right]. \qquad (75)\end{aligned}$$

The coefficient functions $x_{jk}(t,t')$ are determined upon substituting Eqs. (74) and (75) into the integral equations. The procedure results in the following integral equations

$$\begin{aligned}x_{11}(t,t') = &\frac{\mathrm{i}}{M\omega}\sin\omega(t-t') \\ &+ \frac{2}{M\omega}\int_{t'}^{t}\mathrm{d}t_1\int_{t_1}^{t}\mathrm{d}t_2\sin\omega(t_1-t') \\ &\times\ \alpha_i(t_1-t_2)x_{11}(t,t_2), \\ x_{12}(t,t') = &-\mathrm{i}\cos\omega(t-t') \\ &+ \frac{2}{M\omega}\int_{t'}^{t}\mathrm{d}t_1\int_{t_1}^{t}\mathrm{d}t_2\sin\omega(t_1-t') \\ &\times\ \alpha_i(t_1-t_2)x_{12}(t,t_2), \\ x_{21}(t,t') = &\cos\omega(t-t') \\ &- \frac{2}{M\omega}\int_{t'}^{t}\mathrm{d}t_1\int_{0}^{t_1}\mathrm{d}t_2\sin\omega(t_1-t') \\ &\times\ \alpha_i(t_1-t_2)x_{21}(t,t_2), \\ x_{22}(t,t') = &-\frac{\sin\omega(t-t')}{M\omega} \\ &- \frac{2}{M\omega}\int_{t'}^{t}\mathrm{d}t_1\int_{0}^{t_1}\mathrm{d}t_2\sin\omega(t_1-t') \\ &\times\ \alpha_i(t_1-t_2)x_{22}(t,t_2), \\ x_{23}(t,t') = &-\frac{2}{M\omega}\int_{t'}^{t}\mathrm{d}t_1\sin\omega(t_1-t') \\ &\times\left[\int_{0}^{t}\mathrm{d}t_2\alpha_r(t_1-t_2)x_{11}(t,t_2) + \int_{0}^{t_1}\mathrm{d}t_2\alpha_i(t_1-t_2)x_{23}(t,t_2)\right], \\ x_{24}(t,t') = &-\frac{2}{M\omega}\int_{t'}^{t}\mathrm{d}t_1\sin\omega(t_1-t') \\ &\times\left[\int_{0}^{t}\mathrm{d}t_2\alpha_r(t_1-t_2)x_{12}(t,t_2) + \int_{0}^{t_1}\mathrm{d}t_2\alpha_i(t_1-t_2)x_{24}(t,t_2)\right].\end{aligned}$$

Finally one obtains the desired master equation in terms of the above expressions,

$$\begin{aligned}\mathrm{i}\hbar\frac{\mathrm{d}\tilde{\rho}_s(t)}{\mathrm{d}t} &= [\hat{H}_s,\tilde{\rho}_s(t)] + A_1(t)\,[\hat{x},\{\hat{x},\tilde{\rho}_s(t)\}] \\ &\quad + A_2(t)\,[\hat{x},\{\hat{p},\tilde{\rho}_s(t)\}] + A_3(t)\,[\hat{x},[\hat{p},\tilde{\rho}_s(t)]] \\ &\quad + A_4(t)\,[\hat{x},[\hat{x},\tilde{\rho}_s(t)]]\,, \end{aligned} \tag{76}$$

where the coefficient functions are

$$A_1(t) = \int_0^t \mathrm{d}t'\alpha_i(t-t')x_{21}(t,t'),$$

$$A_2(t) = \int_0^t \mathrm{d}t'\alpha_i(t-t')x_{22}(t,t'),$$

$$A_3(t) = \int_0^t \mathrm{d}t'\,[\alpha_r(t-t')x_{11}(t,t')+\alpha_i(t-t')x_{23}(t,t')]\,,$$

$$A_4(t) = \int_0^t \mathrm{d}t'\,[\alpha_r(t-t')x_{12}(t,t')+\alpha_i(t-t')x_{24}(t,t')]\,.$$

The master equation Eq. (76) agrees with that derived by Hu, Paz, and Zhang by virtue of path integral technique [88, 89]. As clarified in Ref. [89], $A_1(t)$ is the coefficient for the frequency shift because $[\hat{x},\{\hat{x},\tilde{\rho}_s(t)\}] = [\hat{x}^2,\tilde{\rho}_s(t)]$, $A_2(t)$ is a quantum dissipation term, $A_3(t)$ reflects the anomalous quantum diffusion, and $A_4(t)$ is the coefficient for the normal quantum diffusion.

Furthermore, the exact master equation for a dissipative harmonic oscillator driven by external time-dependent fields was also conveniently solved with above procedure [101]. In this case, the driving fields mediate an interplay between the system and the bath so that the system is dressed by both the driving and the stochastic fields.

5 Numerical algorithms based on stochastic formulation

5.1 Decomposition of bath response function

When a simple master equation exists, the calculation of the reduced density matrix is straightforward. By contrast, the stochastic simulation is deemed to be less efficient than solving the master equation due to the fluctuations of the stochastic density matrix. Therefore, a deterministic approach is always preferred. However, for a general system a closed set of equations like Eq. (75) cannot be reached because the stochastic average related to the bath-induced noises cannot be solved exactly due to the correlation between the stochastic density matrix $\rho_s(t)$ and random field $\bar{g}(t)$. Any attempt to derive deterministic differential equations based on the stochastic Liouville equation has to find a strategy to represent the average involving the bath-induced noises in Eq. (54).

In this section we show that deterministic differential equations can still be achieved if the response function of the bath can be expanded as

$$\alpha(t) = \sum_j b_j t^{n_j}\mathrm{e}^{-\gamma_j t}. \tag{77}$$

Here γ_j may be complex with positive real part and n_j are non-negative integers. Eq. (77) can be viewed as an expansion of $\alpha(t)$ in terms of the basis functions $\phi_j(t) = t^{n_j}\mathrm{e}^{-\gamma_j t}$, which are related to the orthonormal Laguerre polynomials when the constants γ_j are universal. The response function in Eq. (77) is decomposable such that it can be recast as

$$\alpha(t-s) = \sum_{j,k} c_{j,k}\phi_j(t)\phi_k(s). \tag{78}$$

Furthermore, an arbitrary order derivative of the expansion can also be expressed in terms of these basis functions

$$\frac{\mathrm{d}^n}{\mathrm{d}t^n}\alpha(t) = \sum_j d_j^{(n)}\phi_j(t), \tag{79}$$

where $d_j^{(n)}$ are constants of time. The properties of Eqs. (78) and (79) greatly simplify the derivation of the deterministic equation for the reduced density matrix.

It could be pointed out that Eq. (77) is a general form of the response function for a wide range of model spectral density functions. In many models for the bath, the spectral density function assumes the form of the odd rational function,

$$J(\omega) = \omega\frac{P_K(\omega^2)}{Q_M(\omega^2)}, \tag{80}$$

where $P_K(Q_M)$ is a polynomial of order $K(M)$. The spectral density functions for Ohmic dissipation with the Debye [Eq. (51)] and the algebraic [Eq. (89)] [102] regulation as well as the multiple-mode Brownian oscillator model [85] assume this form. Eq. (34) then can be integrated with contour integration and the contribution of the poles of the spectral density function and the hyperbolic cotangent function results in a form of Eq. (77). Note that when the denominator polynomial $Q_M(x)$ has only simple roots, Eq. (77) will reduce to a summation of exponentials. The integers n_j in Eq. (77) will become non-zero when the polynomial $Q_M(x)$ has multiple roots. Furthermore, the spectral density function may well be approximated with rational functions even if it does not assume the form of odd rational functions. For example, the Ohmic spectral density can be decomposed into shifted Drude–Lorentzian terms [103, 104]. In this case, the corresponding response function is indeed a sum of exponentials.

5.2 Hierarchical approach

In 1978 Shapiro and Loginov proposed the formulae of differentiation to calculate the first order momentum for a stochastic process driven by an Ornstein-Uhlenbeck

noise with a correlation function of a single exponential [105]. Tanimura and Kubo also obtained the Shapiro-Loginov equations when employing the semiclassical approximation for the dissipative dynamics at high temperatures, where the response function of the bath is a single exponential [106]. The low temperature corrections were included soon by Tanimura [107]. Later, our group gave a rigorous derivation of the hierarchical approach through the stochastic formulation.

To derive the hierarchical approach, one again needs to deal with Eq. (54). For a general system the average related to the bath-induced random field $\mathcal{M}\langle\bar{g}(t)\rho_s\rangle$ cannot be solved analytically and one has to resort to the differential equation for its time evolution,

$$\begin{aligned}
&\mathrm{i}\hbar\frac{\mathrm{d}}{\mathrm{d}t}\mathcal{M}\langle\bar{g}(t)\rho_s\rangle\\
&\quad=\mathrm{i}\hbar\mathcal{M}\langle\bar{g}(t)\mathrm{d}\rho_s\rangle/\mathrm{d}t+\mathrm{i}\hbar\mathcal{M}\langle[\mathrm{d}\bar{g}(t)]\rho_s\rangle/\mathrm{d}t\\
&\qquad+\mathrm{i}\hbar\mathcal{M}\langle[\mathrm{d}\bar{g}(t)]\mathrm{d}\rho_s\rangle/\mathrm{d}t\\
&\quad=[\hat{H}_s,\mathcal{M}\langle\bar{g}(t)\rho_s\rangle]+\mathrm{i}\mathcal{M}\langle\bar{g}_1(t)\rho_s\rangle\\
&\qquad+[f(\hat{s}),\mathcal{M}\langle\bar{g}^2(t)\rho_s\rangle]+\alpha_r(0)[f(\hat{s}),\rho_s]\\
&\qquad+\mathrm{i}\alpha_i(0)\{f(\hat{s}),\rho_s\}.
\end{aligned}\tag{81}$$

Here $\bar{g}_1(t)$ is a random field arising from the differentiation of $\bar{g}(t)$

$$\begin{aligned}
\bar{g}_1(t)=\int_0^t&[(\mathrm{d}\mu_{1,\tau}-\mathrm{i}\mathrm{d}\mu_{4,\tau})\dot{\alpha}_r(t-\tau)\\
&+(\mathrm{d}\mu_{2,\tau}+\mathrm{i}\mathrm{d}\mu_{3,\tau})\dot{\alpha}_i(t-\tau)].
\end{aligned}\tag{82}$$

The second identity in Eq. (81) is obtained by using the stochastic Liouville equation Eq. (25) and recognizing the nonanticipating rule Eq. (15). New density matrices $\mathcal{M}\langle\bar{g}^2(t)\rho_s(t)\rangle$ and $\mathcal{M}\langle\bar{g}_1(t)\rho_s(t)\rangle$ appear on the right hand side of this equation. The former originates from the bath-induced field term in the stochastic Liouville equation and the latter comes from the differentiation of the bath-induced field.

To work out a deterministic equation for $\mathcal{M}\langle\bar{g}(t)\rho_s(t)\rangle$, one needs to find the differential equations for the two density matrices $\mathcal{M}\langle\bar{g}^2(t)\rho_s(t)\rangle$ and $\mathcal{M}\langle\bar{g}_1(t)\rho_s(t)\rangle$. This procedure generates new density matrices whose equations of motion involve more terms. However, it will be greatly simplified if the response function can be decomposed in terms of Eq. (77). Originally, only the sum-of-exponential approximation for the bath response function was used for the hierarchical approach. In Ref. [108], we at the first time went beyond this approximation by using a response function related to the Laguerre polynomials

$$\alpha(t)=\mathrm{i}bt\mathrm{e}^{-\Omega t},\tag{83}$$

where b and Ω are real numbers. Very recently, Tang and co-workers suggested an expansion of the bath response function with a complete set of orthonormal functions for the hierarchical scheme [109].

In the following, we will illustrate the derivation of the hierarchical approach with Eq. (83). To include all terms generated in the procedure of differentiation, we introduce the auxiliary density matrices

$$\rho_{m,n}(t)=\mathcal{M}\left\{\bar{g}^m(t)\bar{h}^n(t)\rho_s(t)\right\},\tag{84}$$

with the root entry $\rho_{0,0}(t)$ being the reduced density matrix. Here, the auxiliary stochastic process $\bar{h}(t)$, which accounts the new term other than $\bar{g}(t)$ when substituting Eq. (83) into Eq. (82), is defined as

$$\bar{h}(t)=\int_0^t(\mathrm{d}\mu_{2,\tau}+\mathrm{i}\mathrm{d}\mu_{3,\tau})b\mathrm{e}^{-\Omega(t-\tau)}.\tag{85}$$

The differential equations of the auxiliary density matrices are obtained through the fundamental Itô calculus

$$\begin{aligned}
\mathrm{i}\hbar\dot{\rho}_{m,n}(t)=&-\mathrm{i}\hbar(m+n)\Omega\rho_{m,n}(t)+[\hat{H}_s,\rho_{m,n}(t)]\\
&+[f(\hat{s}),\rho_{m+1,n}(t)]+\mathrm{i}n\hbar b\{f(\hat{s}),\rho_{m,n-1}(t)\}\\
&+\mathrm{i}m\hbar\rho_{m-1,n+1}(t).
\end{aligned}\tag{86}$$

By definition the initial condition is $\rho_{0,0}(0)=\tilde{\rho}_s(0)$ and $\rho_{m,n}(0)=0$ $(m+n\neq 0)$.

Eq. (86) forms a hierarchical structure for the evolution of the auxiliary density matrices. The evolution of the reduced density matrix ($\rho_{0,0}$) involves the density matrix in the first layer, i.e., $\rho_{1,0}$. The auxiliary density matrix in the first layer is coupled to root and those in the second layer, and so forth. Here the auxiliary density matrices with the same value of $m+2n$ form a layer of the hierarchy with the value $m+2n$ indicating the times of differentiation required for the root to access this layer. Thus the value $m+2n$ can be understood as the depth of the auxiliary density matrix $\rho_{m,n}$ and reflects the order of correlation of the noise in the propagation of the reduced density matrix.

The derivation can be extended to a response function with arbitrary number of terms in Eq. (77). For example, with a response function containing three exponentials, one can use three integers to identify the auxiliary density matrices $\rho_{m,n,k}(t)$. Then as depicted in Fig. 5, all the density matrices in the hierarchy are linked to the previous and the next layers through a pyramid-like structure.

Actually the hierarchy approach is a scheme to embed a non-Markovian system in a larger, possibly infinite Markovian system and the memory effects are characterized by the auxiliary terms. In other words, it converts an integro-differential equation with a degenerate kernel to infinite number of hierarchy equations. We would like to point out that the auxiliary density matrices also carry the information for the bath and have physical meaning instead of being pure mathematical intermediate entities. For example, the auxiliary density matrices in the first layer are directly related to the transport

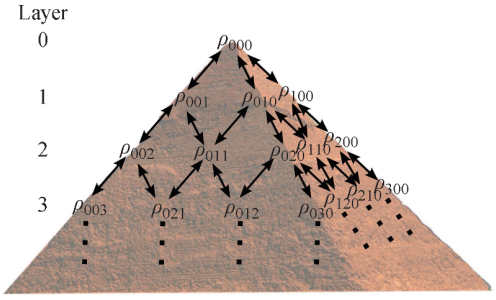

Fig. 5 The pyramid-like structure of the auxiliary density matrices in the hierarchical evolution for response function containing three exponentials.

current in fermionic systems [110].

5.3 Performance of hierarchical approach

The hierarchy equation Eq. (86) is an infinite-dimensional ordinary differential equation. It is an unattainable yet unnecessary work to handle an infinite system exactly in numerical simulations. Normally, the deeper the layer is, the less impact it has on the evolution of the reduced density matrix. In practice, one can safely truncate the hierarchy equation to the Kth layer with a sufficiently large integer K. That is, all terms $\rho_{m,n,k}(t)$ with $m+n+k > K$ are set to zero. The level of truncation K depends on the system-bath coupling strength. The stronger the coupling is, the larger value of K has to be used for the truncation. In the numerical simulations we will choose the minimum value K_{min} such that the differences between the results with truncation of K_{min} and $K_{min}+1$ are smaller than a preselected criteria but those between K_{min} and $K_{min}-1$ are not.

To verify this point we will check the performance of the hierarchical approach for the dissipated symmetric two-level system Eq. (50). For the clarity of showing the impact of parameters on the performance of the hierarchy equation, the response function is assumed to take a single exponential,

$$\alpha(t) = 0.5\eta\omega_c^2(0.5\cot(\beta\omega_c/2) - \mathrm{i})\exp(-\omega_c|t|), \quad (87)$$

which is essentially the first term in the response function Eq. (52) by ignoring contributions from all Matsubara frequencies. Here we set $\beta = 0.5$ and explore how the level of truncation depends on the dissipation strength η with a cut-off $\omega_c = 4$. Figure 6(a) shows the dissipation strength dependence of the truncation level K_{min} with tolerances of 2×10^{-3} and 10^{-4}. The differences in the results with a maximum deviation of 2×10^{-3} cannot be recognized with naked eye if they are plotted on top of each other. It verifies that in general the hierarchy equation can converge when we include more and more layers. When the tolerance decreases by a factor of

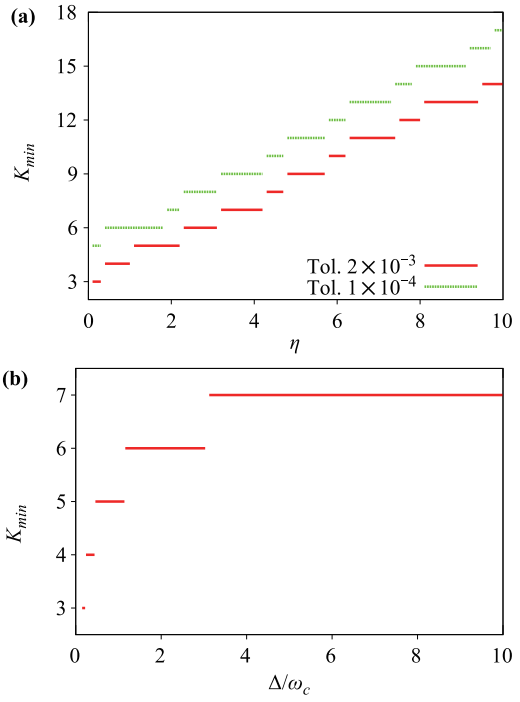

Fig. 6 The relation between the truncation level K_{min} and **(a)** the dissipation strength η with $\omega_c = 4\Delta$ for the tolerance of 2×10^{-3} and 10^{-4}, and **(b)** the memory time with $\eta = 0.5$ for the TLS with response function Eq. (87) at temperature $T = 2\Delta$.

20, usually we have to increase the truncation level by one or two. With a properly chosen truncation level, we even can obtain numerically exact results with machine accuracy of the double precision.

Because the hierarchy approach gives the finite memory time corrections to the Markovian approximation, we expect that the truncation level would be small for short bath memory times. Again, we will use the symmetric two-level system Eq. (50) and the single exponential response function Eq. (87) to illustrate this point. Here $\beta = 2\Delta$, $\eta = 0.5$ are fixed and ω_c varies from 0.1 to 70. The results are plotted in Fig. 6(b). It shows an overall monotonic increase of the truncation level with respect to the memory time (measured by Δ/ω_c). When the memory time is around 0.15, $K_{min} = 3$ is already sufficient to produce the accuracy of 0.002. The truncation level gradually increases up to seven when the memory goes to 10.

In the hierarchy equation, the auxiliary density matrix $\rho_{m,n}$ is damped by the factor $(m+n)\Omega$. The matrices with large damping factors will decay fast in time propagation. There exist alternative truncation schemes based on this fact. Shi and co-workers introduced a filtering scheme after rescaling the auxiliary density matrices that automatically truncates the hierarchy with a preselected tolerance [111]. This truncation scheme may significantly reduce the number of auxiliary den-

sity matrices and speed up the numerical simulation of the hierarchical approach.

The computational effort, such as computer memory and CPU time required for the numerical simulation, directly depends on the number of auxiliary density matrices in the hierarchy. The jth layer has $(j+N-1)!/(j!(N-1)!)$ auxiliary density matrices for N exponentials. The total number of density matrices for K layers is

$$L(K,N)=\sum_{j=0}^{K}\frac{(j+N-1)!}{j!(N-1)!}=\frac{(K+N)!}{K!N!}. \tag{88}$$

Therefore, the computational effort scales exponentially with respect to the number of terms approximating the response function. It is appreciated to reduce the number of exponentials decomposing the response function without loss of accuracy. For this purpose, Yan and coworkers used the Padé approximant of the Bose/Fermi function to obtain accurate approximation for the response function with a few exponentials [112, 113].

Here the hierarchy equation is derived based on the stochastic decoupling for the reduced density matrix. Similar hierarchy equations were derived for multi-time correlation functions [114] and for diffusively driven quantum systems [115]. Very recently, de Vega suggested another form of hierarchical equations [116]. Zhou and co-workers also derived non-Markovian quantum Bloch equations in the hierarchical form [117].

Now the hierarchical approach has become a standard tool for the simulation of the non-Markovian dynamics. It has been applied to the study of quantum coherence in a photosynthetic system [118], the dissipative two-exciton dynamics in molecular aggregate [119], the exciton Seebeck effect in molecular systems [120], the exciton interference [121], two-dimensional electronic spectra [122], Kondo effects in driven strongly correlated quantum dots [123], to name but only a few.

As numerical examples, the hierarchical simulations of the spin-boson model Eq. (50) are performed assuming the Ohmic spectral density function with the Debye regulation Eq. (51). We will explore the dynamics with a broad range of the dissipation strength η and the frequency cut-off ω_c. As discussed above, only the first N_e exponentials in the response function Eq. (52) need to be incorporated into the hierarchy with a finite level of truncation K_{min}.

Figure 7 displays the dynamics of the TLS with a fast bath ($\omega_c=5\Delta$) at temperature $T=2\Delta$. It shows that for weak dissipation with $\eta=0.4$, clear quantum coherence is manifested by the oscillation of the population difference. The calculation converges with four exponentials up to the seventh order. When the dissipation is strong, i.e., $\eta=8$, the system returns to the equilibrium without oscillation, but with a longer relaxation time. In this case, we have to incorporate six

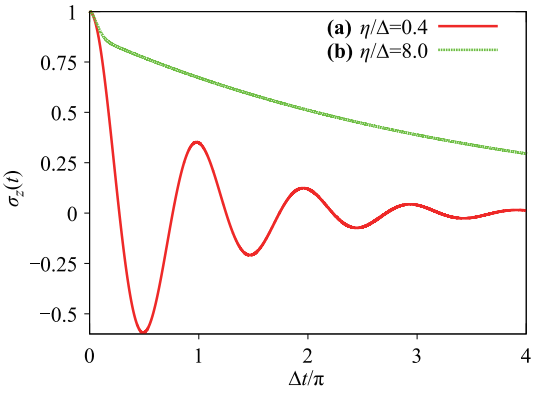

Fig. 7 The time evolution of the population difference for the TLS with a relative large cut-off $\omega_c=5\Delta$ at temperature $T=2\Delta$ for **(a)** $\eta=0.4$ and **(b)** $\eta=8$. The hierarchy parameters are $N_e=4$, $K_{min}=7$ for (a) and $N_e=6$, $K_{min}=9$ for (b).

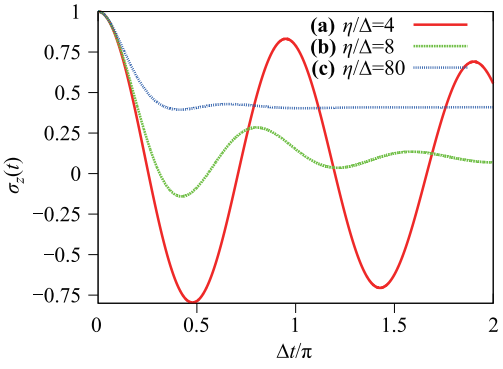

Fig. 8 The time evolution of the population difference for the TLS with a small cut-off $\omega_c=0.25\Delta$ at temperature $T=0.5\Delta$ for **(a)** $\eta=4$, $N_e=4$, $K_{min}=6$; **(b)** $\eta=8$, $N_e=6$, $K_{min}=9$; and **(c)** $\eta=80$, $N_e=7$, $K_{min}=25$.

exponentials and truncate the hierarchy at the ninth order.

The scenario changes for a TLS with a slow bath ($\omega_c=0.25\Delta$) at a lower temperature $T=0.5\Delta$. As depicted in Fig. 8, the system is slightly damped for a rather large coupling constant $\eta=4$. The coherence is still observable with a strength as large as $\eta=80$.

6 Hybrid stochastic-hierarchical equation

For the dissipative harmonic oscillator, either classical or quantum, as the dissipation increases, the motion will change from coherence to exponential decay. For the undissipated two-level system, the dynamics exhibits coherence as the system changes from one localized state to the other periodically. Under weak to intermediate dissipation, the coherence between the two localized states will be destroyed and the zero-temperature dy-

namical behavior of the spin-boson model is expected to exhibit the similar coherence-to-decoherence transition. However, the dissipated two-level system is nonlinear and there exists a critical value for the dissipation strength beyond which the dynamics is frozen. In this case the dynamical phase transition occurs for the spin-boson model, which is nothing but the localization [124].

It remains a challenge for theorists to simulate non-Markovian quantum dissipative dynamics under strong dissipation at zero temperature. Both the stochastic and hierarchical approaches have disadvantages in numerical simulations of the low temperature dynamics. On one side, the stochastic Liouville equation is suitable for the dynamics at arbitrary temperatures under weak to intermediate dissipation. The performance is mainly degraded by the imaginary part of the response function which makes the stochastic density matrix non-Hermitian and non-norm-conserving. On the other side, hierarchical approach is numerically efficient for intermediate to strong dissipation. However, when the temperature becomes low, many terms have to be included in the expansion of the real part of the response function. Therefore, the treatment of the real part of the response function makes the hierarchical approach only suitable for medium to high temperatures. Based on the above analysis, a natural question arises: Can we combine the hierarchical and stochastic schemes to use their advantages and circumvent their disadvantages to achieve an efficient numerical method for dynamics under strong dissipation at low temperatures or even at zero temperature?

This question led to the hybrid stochastic-hierarchical equations [108, 125]. The original idea was to use the mixed random-deterministic (MRD) scheme to deal with the imaginary part of the response function by the hierarchical approach and to handle the real part with the stochastic method [108]. To be specific, the stochastic average of Eq. (25) with respect to w_2 is tackled with the hierarchical approach and that with respect to w_1 is maintained with the stochastic scheme. It is successful to calculate long-time dynamics for weak to moderate dissipation at zero temperature but fails for strong dissipation. A natural remedy is the introduction of the flexible random-deterministic (FRD) scheme where a few exponentials are extracted from the real part of the response function and tackled with the hierarchical approach [125]. By doing so, the rest of the response function which needs to be dealt with by the random scheme is much smaller. Consequently, the flexible scheme is efficient both in producing the random average and in representing the response function. Its numerical performance is greatly improved and suitable for the zero temperature dynamics under strong dissipation.

To explore the performance of these methods we use the dissipated symmetric two-level system under Ohmic dissipation with a polynomial cut-off [102]

$$J(\omega) = 2\pi\eta\omega/\left[1+(\omega/\omega_c)^2\right]^2, \tag{89}$$

where η is the Kondo parameter characterizing the dissipation strength. The imaginary part of the response function is an exponentially weighted polynomial

$$\alpha_i(t) = -\frac{1}{2}\pi\eta\omega_c^3 t\mathrm{e}^{-\omega_c t}, \tag{90}$$

which can be effectively tackled with the hierarchical approach.

The dynamics of the dissipative system at zero temperature for the Kondo parameter $\alpha = 0.1$–0.5 and the cut-off $\omega_c = 10\Delta$ were simulated with the mixed random-deterministic scheme. The results shown in Fig. 9 display a clear pattern of the transition from coherent to incoherent motion. The population differences exhibit obvious coherence when the dissipation strength is less than 0.5 and follow an exponential decay for $\alpha = 0.5$.

To scrutinize the dynamics at zero temperature, we also carried out the simulations with the mixed random-deterministic scheme for the population differences with cut-offs of 20Δ and 40Δ. Here we present the results for $\alpha = 0.1$ as an example. As shown in Fig. 10, the results for different frequency cut-offs fit together once the time axis is rescaled by the renormalization frequency

$$\Delta_r = \Delta\left(\frac{\Delta}{\omega_c}\right)^{\alpha/(1-\alpha)}. \tag{91}$$

This feature implies that the frequency cut-off ω_c only comes into the time scale of the dynamics through Δ_r for large cut-offs. In this case, the scaling limit is almost reached when $\omega_c = 10$. The results based on the noninteracting-blip approximation (NIBA) are also plotted in this figure. For such weak dissipation the noninteracting-blip approximation gives almost exact results. It produces noticeable and even significant errors for stronger dissipation, except for the case with $\alpha = 0.5$ [125].

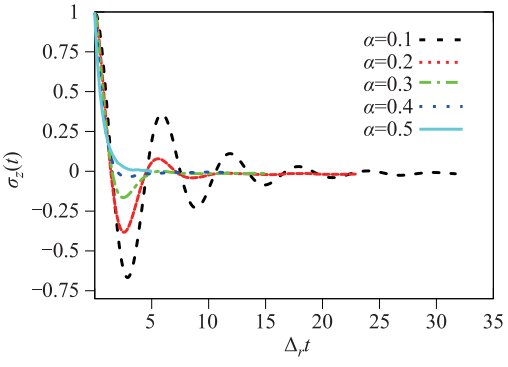

Fig. 9 The coherent dynamics of the spin-boson model at zero temperature for various dissipation strength α simulated with the mixed random-deterministic scheme. The frequency cut-off is $\omega_c = 10\Delta$.

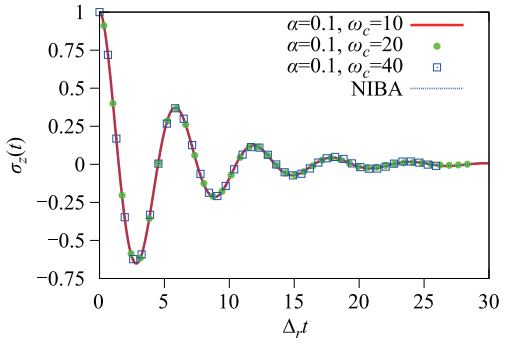

Fig. 10 The scaling limit of the spin-boson model at zero temperature for dissipation strength $\alpha = 0.1$ simulated with the mixed random-deterministic scheme. NIBA gives almost exact results for this case.

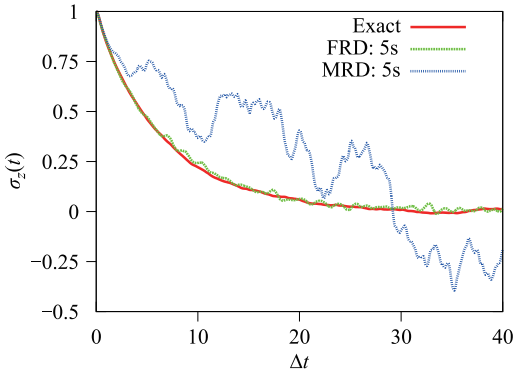

Fig. 11 The dynamics of the spin-boson model at zero temperature for dissipation strength $\alpha = 0.5$. The frequency cut-off is $\omega_c = 10\Delta$. Solid line shows the converged results with the mixed random-deterministic scheme. The results for the flexible scheme were calculated with a common desktop within five seconds. A 5-seconds simulation of the mixed random-deterministic scheme is also shown for the comparison of the numerical efficiency.

The results for $\alpha = 0.2 - 0.5$ with different cut-offs confirm the scaling behavior. For $\alpha = 0.5$, the population difference at long times exhibits an exponential decay with respect to the time rescaled by the renormalization frequency Δ_r. This exponential decay agrees with the theoretical prediction from the noninteracting-blip approximation [32], which becomes exact for an infinite frequency cut-off for $\alpha = 0.5$.

The mixed random-deterministic scheme becomes inefficient under strong dissipation and one has to resort to the flexible scheme. Fig. 11 presents a comparison of the efficiency between the mixed and flexible random-deterministic schemes for the case with $\alpha = 0.5$. It takes the mixed scheme more than one day to obtain the converged results with a common desktop computer. But the flexible scheme yields reasonable results within five seconds with the same computer. For a clear comparison the results based on the mixed random-deterministic scheme within five seconds are also demonstrated, which display a dramatic deviation from the ensemble average.

The flexible random-deterministic scheme allows the exploration of the dynamics for $\alpha > 0.5$ within a reasonably short amount of time. It will take several days to several weeks to simulate the dynamics with $0.5 < \alpha \leq 0.8$. Figure 12 depicts the results for $\alpha = 0.6$. Other cases assume similar features and are not shown here. Again the results based on the noninteracting-blip approximation are compared, which are only good at short times and become qualitatively correct for long times for such strong dissipations. In these cases the population differences follow an exponential decay after an initial quick drop. But now the frequency cut-off dependency is different to that in the weak dissipation cases with $\alpha \leq 0.5$. As revealed by panel (b), the quantities $\ln[\sigma_z(t)]$ with different frequency cut-offs fit together if the time is rescaled with $1/\omega_c$ for large cut-off. For such strong dissipation, the scaling limit is reached around $\omega_c = 20\Delta$, which is later than $\omega_c = 10\Delta$ for a weak dissipation with $\alpha = 0.1$. Once the scaling limit is maintained, the quantity $\ln[\sigma_z(t)]$ shows a linear dependence on $\Delta(\Delta/\omega_c)t$. It strongly suggests that there is a phase transition at $\alpha = 0.5$ for the spin-boson model at zero temperature. In the scaling limit $\omega_c/\Delta \to \infty$, the dynamics changes from coherent motion for $\alpha < 0.5$ to exponential decay for $0.5 \leq \alpha < 1.0$. Accordingly, the scaling factor changes from Δ_r to $\Delta(\Delta/\omega_c)$. The

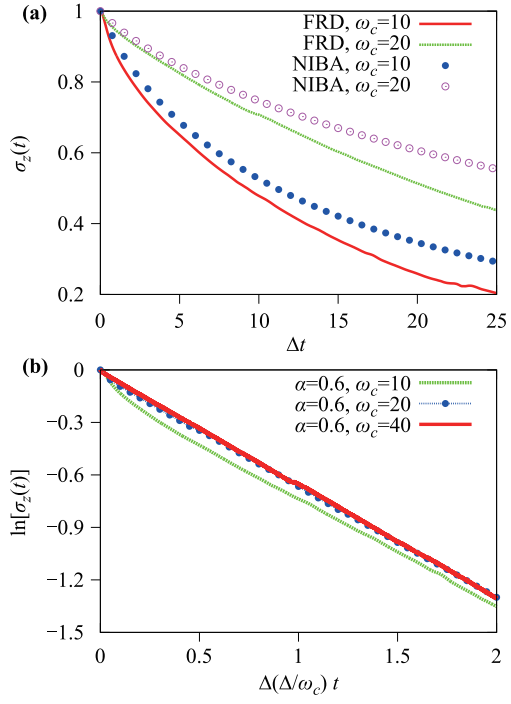

Fig. 12 The dynamics of the spin-boson model at zero temperature for dissipation strength $\alpha = 0.6$ with different frequency cut-off. **(a)** The comparison between the FRD and NIBA; **(b)** The scaling limit for the FRD simulations.

transition to localization at $\alpha = 1.0$ is also predicted by various analytic theories [32, 34] in the limit $\omega_c/\Delta \to \infty$. These results are summarized in Fig. 13.

One may introduce a decay rate as

$$\kappa = -\omega_c \lim_{t\to t_c} \frac{\mathrm{d}\ln[\sigma_z(t)]}{\mathrm{d}t}, \tag{92}$$

with a sufficiently large time t_c. The results of the decay rates for the Kondo parameters $0.5 \le \alpha \le 0.8$ are presented in Fig. 14. Though the existence of the exponential decay could be explained by conformal field theory [34, 126], the predicted results are different from the current simulations. The decay rate decreases as the dissipation becomes stronger. Interestingly, the logarithm of the decay rate shows a linear dependence on the dissipation strength.

7 Summary and perspectives

The past two decades have witnessed an increasing popularity of stochastic simulations of quantum dissipative dynamics. Particularly, the influence functional within the framework of linear dissipation can be naturally reconstructed with the random average by introducing Gaussian random forces to the system. Thanks to the Hubbard–Stratonovich transformation, we have decoupled the system and the bath. The original system-bath coupling is converted into the correlation induced by the motion of the stochastic system and the bath under the influence of the common white noise forces. The sole effect of the bath is to provide a random field on the evolution of the system. For the linear dissipation model, the motion of the bath is exactly known and the bath-induced random field can be worked out. Thus a stochastic Liouville equation can be derived for the reduced dynamics without explicit treatment of the bath.

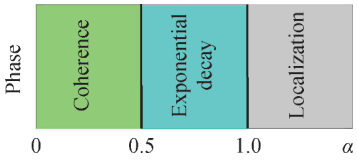

Fig. 13 The phase diagram for the spin-boson model at zero temperature in the scaling limit $\omega_c/\Delta \to \infty$.

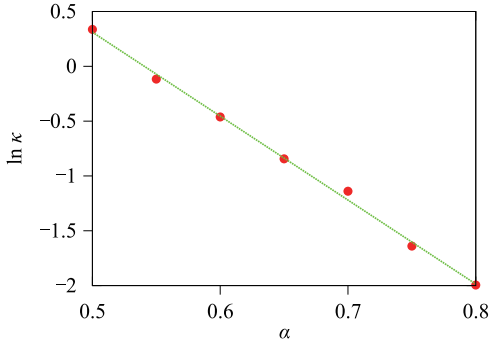

Fig. 14 The logarithm of the decay rate as the function of the dissipation strength for the spin-boson model at zero temperature. Symbols are calculated results and the line is for the guide of the eye with a linear function $\ln\kappa = 4.14 - 7.66\alpha$.

The final stochastic Liouville equation does not preserve hermicity, norm-conserving, or positivity, which affects its numerical performance. To have a better numerical performance, a Hermitian scheme has also been developed. The stochastic simulation is simple, easy to be implemented and suitable for numerical simulations of dissipative dynamics with weak to intermediate coupling strength at arbitrary temperatures.

The stochastic scheme can also serve as a useful theoretical tool to derive deterministic master equation. For the analytically solvable models and for the memoryless bath, we can carry out the random average analytically to achieve the exact master equation. The procedure for general systems with arbitrary bath response function is not closed. However, if the response function is a degenerate kernel, i.e., decomposable in terms of exponentials or exponential-weighted Laguerre polynomials, an efficient hierarchy approach can be developed, where the memory effects is characterized by the auxiliary density matrices.

But at low temperatures, the response function of the bath must be approximated with many terms and the hierarchical simulations may become prohibitively expansive. In these cases, we can combine the deterministic and stochastic schemes to handle part of the response function with the hierarchical approach and the rest with the stochastic scheme. Such hybrid stochastic-hierarchical equations exploit the advantages of the stochastic and hierarchical schemes and are suitable for the lower temperature dynamics with strong dissipation.

As described above, the Hubbard-Stratonovich transformation provides us a machinery to decouple the interaction between different physical variables via introducing white noises. It is, in principle, a (at least partial) cure for the curse of dimensionality, yet would not become powerful unless the average of the concomitant stochastic evolution is feasibly obtained. We see that it works well for a bosonic bath with linear couplings to the system and the bath-induced stochastic field can be derived in a closed form. For a general bath, however, no analytic results are available. It is no doubt that obtaining a reasonably accurate bath-induced stochastic field is a challenging task.

It is really ideal if the master equation that a dissipative system obeys can be derived. Then it would be easier to use such a deterministic equation to reveal the dynamical features of quantum dissipation. Unfortunately, even if the induced stochastic field is known for the linear bath and the stochastic Liouville equation has been determined, the master equation for the nonlinear dis-

sipative system is elusive. The difficulty is rooted at the correlation between the bath-induced stochastic field and the evolution of the system. Except for the case of weak dissipation in which a reliable perturbation treatment may lead a master equation, it is hardly possible to find a deterministic equation of motion with general dissipation. Although numerical simulations based on the stochastic Liouville equations are applicable, the computational cost would increase rapidly as the dissipation gets stronger and the statistical error would eventually be uncontrollable. This problem may be alleviated by using a nonlinear but norm-conserved stochastic Liouville equation instead of the linear one, but nonlinearity may also cause numerical instability.

The lesson we have learnt is that stochastic simulation is a general approach with low efficiency while deterministic method is highly effective but limited to specific systems. The mixed stochastic-deterministic technique enjoys some success in solving the dynamics of the spin-boson model, yet more effective numerical algorithm with more flexibility and feasibility, addressing general quantum dissipative dynamics is yet to be developed.

From a fundamental perspective, because many macroscopic effects ranging from pure physical such as turbulence, phase transition to biological such as memory and so on are only possible within dissipative systems, to reveal the underlying mechanism of these emergent effects needs conceptual as well as theoretical advances. In a recent article Whitesides listed how dissipative systems work as the third new class of problems for chemists [127]. As he pointed, "Studying dissipative systems has, of course, been a subject of physical science for decades, but, unlike equilibrium systems, understanding dissipative systems—both theoretically and empirically—is still at the very beginning". More fruitful emergent phenomena such as quantum phase transition, a behavior change from delocalized quantum world to the localized classical one, may undergo in quantum dissipative systems and still await for exploration [128].

Acknowledgements The authors thank Yun Zhou for his generous help with figure plotting. This work was supported by the National Natural Science Foundation of China (Grant Nos. 21421003 and 21373064) and the 973 Program of the Ministry of Science and Technology of China (Grant No. 2013CB834606).

References

1. R. E. Bellman, *Dynamic Programming* (Princeton University Press, Princeton, 1957)
2. H. J. Berendsen, *Simulating the Physical World: Hierarchical Modeling from Quantum Mechanics to Fluid Dynamics* (Cambridge University Press, Cambridge, 2007)
3. A. O. Caldeira, *An Introduction to Macroscopic Quantum Phenomena and Quantum Dissipation* (Cambridge University Press, Cambridge, 2014)
4. S. Chandrasekhar, Stochastic problems in physics and astronomy, *Rev. Mod. Phys.* **15**, 1 (1943)
5. S. Dattagupta, *Relaxation Phenomena in Condensed Matter Physics* (Academic Press, Orlando, 2012)
6. B. J. Berne, G. Cicootti, and D. F. Coker, eds., *Classical and Quantum Dynamics in Condensed Phase Simulations*, Computer Simulation of Rare Events and the Dynamics of Classical and Quantum Condensed-Phase Systems (World Scientific, Singapore, 1998)
7. W. Ji, H. Xu, and H. Guo, Quantum description of transport phenomena: Recent progress, *Front. Phys.* **9**, 671 (2014)
8. A. Einstein, Über die von der molekularkinetischen theorie der wärme geforderte bewegung von in ruhenden flüssigkeiten suspendierten teilchen, *Ann. Phys.* **322**, 549 (1905)
9. M. von Smoluchowski, Zur kinetischen theorie der Brownschen molekularbewegung und der suspensionen, *Ann. Phys.* **326**, 756 (1906)
10. M. Scott, *Applied Stochastic Processes in Science and Engineering* (University of Waterloo, Waterloo, 2013)
11. C. Gardiner, *Handbook of Stochastic Methods*, 3rd ed. (Springer, Berlin, 2004)
12. N. van Kampen, *Stochastic Processes in Physics and Chemistry*, 3rd ed. (Elsevier, Amsterdam, 2007)
13. J. B. Johnson, Thermal agitation of electricity in conductors, *Phys. Rev.* **32**, 97 (1928)
14. H. Nyquist, Thermal agitation of electric charge in conductors, *Phys. Rev.* **32**, 110 (1928)
15. P. Langevin, Sur la théorie du mouvement Brownien, *C. R. Acad. Sci. Paris* **146** (1908)
16. D. S. Lemons and A. Gythiel, Paul Langevin's 1908 paper "on the theory of Brownian motion" ["sur la théorie du mouvement brownien," C. R. Acad. Sci. (Paris) 146, 530-533 (1908)], *Am. J. Phys.* **65**, 1079 (1997)
17. A. D. Fokker, Die mittlere energie rotierender elektrischer dipole im strahlungsfeld, *Ann. Phys.* **348**, 810 (1914)
18. M. Planck, An essay on statistical dynamics and its amplification in the quantum theory, *Sitz. Ber. Preuß. Akad. Wiss.* **325**, 324 (1917)
19. A. Kolmogoroff, Über die analytischen methoden in der wahrscheinlichkeitsrechnung, *Math. Ann.* **104**, 415 (1931)
20. H. Risken, *Fokker-Planck Equation*, Springer Series in Synergetics (Springer, Berlin, 1984)
21. G. E. Uhlenbeck and L. S. Ornstein, On the theory of the Brownian motion, *Phys. Rev.* **36**, 823 (1930)
22. H. A. Kramers, Brownian motion in a field of force and the diffusion model of chemical reactions, *Physica* **7**, 284 (1940)
23. P. Hänggi, P. Talkner, and M. Borkovec, Reaction-rate theory: fifty years after Kramers, *Rev. Mod. Phys.* **62**, 251 (1990)
24. R. Kubo, A stochastic theory of line shape, *Adv. Chem. Phys.* **15**, 101 (1969)
25. H. B. Callen and T. A. Welton, Irreversibility and generalized noise, *Phys. Rev.* **83**, 34 (1951)
26. R. Kubo, The fluctuation-dissipation theorem, *Rep.*

Prog. Phys. **29**, 255 (1966)
27. S. Nakajima, On quantum theory of transport phenomena: Steady diffusion, *Prog. Theor. Phys.* **20**, 948 (1958)
28. R. Zwanzig, Ensemble method in the theory of irreversibility, *J. Chem. Phys.* **33**, 1338 (1960)
29. G. W. Ford, J. T. Lewis, and R. F. O'Connell, Quantum Langevin equation, *Phys. Rev. A* **37**, 4419 (1988)
30. M. C. Wang and G. E. Uhlenbeck, On the theory of the Brownian motion II, *Rev. Mod. Phys.* **17**, 323 (1945)
31. H.-P. Breuer and F. Petruccione, *Theory of Open Quantum Systems* (Oxford University Press, Oxford, 2002)
32. A. J. Leggett, S. Chakravarty, A. T. Dorsey, M. P. A. Fisher, A. Garg, and W. Zwerger, Dynamics of the dissipative two-state system, *Rev. Mod. Phys.* **59**, 1 (1987)
33. P. Hänggi and G. Ingold, Fundamental aspects of quantum Brownian motion, *Chaos* **15**, 026105 (2005)
34. U. Weiss, *Quantum Dissipative Systems*, 3rd ed., Series in Modern Condensed Matter Physics, Vol. 13 (World Scientific, Singapore, 2008)
35. A. Caldeira and A. Leggett, Quantum tunnelling in a dissipative system, *Ann. Phys.* **149**, 374 (1983)
36. R. Feynman and F. Vernon Jr., The theory of a general quantum system interacting with a linear dissipative system, *Ann. Phys.* **24**, 118 (1963)
37. J. Cao, L. W. Ungar, and G. A. Voth, A novel method for simulating quantum dissipative systems, *J. Chem. Phys.* **104**, 4189 (1996)
38. J. T. Stockburger and C. H. Mak, Dynamical simulation of current fluctuations in a dissipative two-state system, *Phys. Rev. Lett.* **80**, 2657 (1998)
39. J. T. Stockburger and H. Grabert, Exact c-number representation of non-markovian quantum dissipation, *Phys. Rev. Lett.* **88**, 170407 (2002)
40. W. Koch, F. Großmann, J. T. Stockburger, and J. Ankerhold, Non-Markovian dissipative semiclassical dynamics, *Phys. Rev. Lett.* **100**, 230402 (2008)
41. L. Diósi and W. T. Strunz, The non-Markovian stochastic schrödinger equation for open systems, *Phys. Lett. A* **235**, 569 (1997)
42. L. Diósi, N. Gisin, and W. T. Strunz, Non-Markovian quantum state diffusion, *Phys. Rev. A* **58**, 1699 (1998)
43. W. T. Strunz, L. Diósi, and N. Gisin, Open system dynamics with non-Markovian quantum trajectories, *Phys. Rev. Lett.* **82**, 1801 (1999)
44. W. T. Strunz, L. Diósi, N. Gisin, and T. Yu, Quantum trajectories for Brownian motion, *Phys. Rev. Lett.* **83**, 4909 (1999)
45. T. Yu, Non-markovian quantum trajectories versus master equations: Finite-temperature heat bath, *Phys. Rev. A* **69**, 062107 (2004)
46. X. Zhao, J. Jing, B. Corn, and T. Yu, Dynamics of interacting qubits coupled to a common bath: Non-markovian quantum-state-diffusion approach, *Phys. Rev. A* **84**, 032101 (2011)
47. H. Breuer, Exact quantum jump approach to open systems in bosonic and spin baths, *Phys. Rev. A* **69**, 022115 (2004)
48. E. Calzetta, A. Roura, and E. Verdaguer, Stochastic description for open quantum systems, *Physica A* **319**, 188 (2003)
49. J. Shao, Decoupling quantum dissipation interaction via stochastic fields, *J. Chem. Phys.* **120**, 5053 (2004)
50. J. T. Stockburger and H. Grabert, Non-Markovian quantum state diffusion, *Chem. Phys.* **268**, 249 (2001)
51. M. Suzuki, Generalized trotter's formula and systematic approximants of exponential operators and inner derivations with applications to many-body problems, *Commun. Math. Phys.* **51**, 183 (1976)
52. D. Gatarek and N. Gisin, Continuous quantum jumps and infinite£dimensional stochastic equations, *J. Math. Phys.* **32**, 2152 (1991)
53. A. O. Caldeira and A. J. Leggett, Path integral approach to quantum Brownian motion, *Physica A* **121**, 587 (1983)
54. W. H. Louisell, *Quantum Statistical Properties of Radiation* (Wiley, New York, 1973)
55. W. Magnus, On the exponential solution of differential equations for a linear operator, *Commun. Pure Appl. Math.* **7**, 649 (1954)
56. D. Finkelstein, On relations between commutators, *Commun. Pure Appl. Math.* **8**, 245 (1955)
57. E. H. Wichmann, Note on the algebraic aspect of the integration of a system of ordinary linear differential equations, *J. Math. Phys.* **2**, 876 (1961)
58. G. H. Weiss and A. A. Maradudin, The baker-hausdorff formula and a problem in crystal physics, *J. Math. Phys.* **3**, 771 (1962)
59. A. Murua, The hopf algebra of rooted trees, free lie algebras, and lie series, *Found. Comput. Math.* **6**, 387 (2006)
60. Y.-A. Yan and Y. Zhou, Hermitian non-Markovian stochastic master equations for quantum dissipative dynamics, *Phys. Rev. A* **92**, 022121 (2015)
61. J. Shao, Rigorous representation and exact simulation of real gaussian stationary processes, *Chem. Phys.* **375**, 378 (2010)
62. R. B. Davies and D. S. Harte, Tests for hurst effect, *Biometrika* **74**, 95 (1987)
63. A. T. A. Wood and G. Chan, Simulation of stationary gaussian processes in $[0,1]^d$, *J. Comp. Graph. Stat.* **3**, 409 (1994)
64. G. Chan and A. Wood, Algorithm AS 312 - An algorithm for simulating stationary gaussian random fields, *App. Stat.* **46**, 171 (1997)
65. G. Chan and A. T. A. Wood, Simulation of stationary gaussian vector fields, *Stat. Comp.* **9**, 265 (1999)
66. C. M. Caves, K. S. Thorne, R. W. P. Drever, V. D. Sandberg, and M. Zimmermann, On the measurement of a weak classical force coupled to a quantum-mechanical oscillator. I. issues of principle, *Rev. Mod. Phys.* **52**, 341 (1980)
67. D. Mozyrsky and V. Privman, Measurement of a quantum system coupled to independent heat-bath and pointer modes, *Mod. Phys. Lett. B* **14**, 303 (2000)
68. J. Shao, M. Ge, and H. Cheng, Decoherence of quantum-nondemolition systems, *Phys. Rev. E* **53**, 1243 (1996)
69. P. Schramm and H. Grabert, Effect of dissipation on squeezed quantum fluctuations, *Phys. Rev. A* **34**, 4515 (1986)
70. P. E. Kloeden and E. Platen, *Numerical Solution of Stochastic Differential Equations*, 2nd ed. (Springer-

Verlag, Berlin, 1995)
71. V. May and O. Kühn, *Charge and Energy Transfer Dynamics in Molecular Systems*, 3rd ed. (WILEY-VCH, Weinheim, 2010)
72. M. Nielsen and I. Chuang, *Quantum Computation and Quantum Information* (Cambridge University Press, Cambridge, 2000)
73. R. Schatten, *Norm Ideals of Completely Continuous Operators*, Ergebnisse der Mathematik und ihrer Grenzgebiete, Neue Folge, Heft 27. (Springer-Verlag, Berlin-Göttingen-Heidelberg, 1960)
74. H.-P. Breuer, E.-M. Laine, and J. Piilo, Measure for the degree of non-markovian behavior of quantum processes in open systems, *Phys. Rev. Lett.* **103**, 210401 (2009)
75. Á. Rivas, S. F. Huelga, and M. B. Plenio, Quantum non-Markovianity: characterization, quantification and detection, *Rep. Prog. Phys.* **77**, 094001 (2014)
76. A. Brissaud and U. Frisch, Solving linear stochastic differential equations, *J. Math. Phys.* **15**, 524 (1974)
77. V. I. Klyatskin, *Dynamics of Stochastic Systems* (Elsevier Science, Amsterdam, 2005)
78. M. Ban, S. Kitajima, and F. Shibata, Reduced dynamics and the master equation of open quantum systems, *Phys. Lett. A* **374**, 2324 (2010)
79. E. Novikov, Functionals and the random-force method in turbulence theory, *Sov. Phys. JETP* **20**, 1290 (1965)
80. J. Cao, A phase-space study of Bloch-Redfield theory, *J. Chem. Phys.* **107**, 3204 (1997)
81. C. Fleming, A. Roura, and B. Hu, Exact analytical solutions to the master equation of quantum Brownian motion for a general environment, *Ann. Phys.* **326**, 1207 (2011)
82. H. Dekker, Quantization of the linearly damped harmonic oscillator, *Phys. Rev. A* **16**, 2126 (1977)
83. H. Dekker, Classical and quantum mechanics of the damped harmonic oscillator, *Phys. Rep.* **80**, 1 (1981)
84. F. Haake and R. Reibold, Strong damping and low-temperature anomalies for the harmonic oscillator, *Phys. Rev. A* **32**, 2462 (1985)
85. H. Grabert, P. Schramm, and G.-L. Ingold, Quantum Brownian motion: The functional integral approach, *Phys. Rep.* **168**, 115 (1988)
86. W. G. Unruh and W. H. Zurek, Reduction of a wave packet in quantum Brownian motion, *Phys. Rev. D* **40**, 1071 (1989)
87. V. Ambegaokar, Dissipation and decoherence in a quantum oscillator, *J. Stat. Phys.* **125**, 1183 (2006)
88. B. L. Hu, J. P. Paz, and Y. Zhang, Quantum Brownian motion in a general environment: Exact master equation with nonlocal dissipation and colored noise, *Phys. Rev. D* **45**, 2843 (1992)
89. B. L. Hu, J. P. Paz, and Y. Zhang, Quantum Brownian motion in a general environment. II. nonlinear coupling and perturbative approach, *Phys. Rev. D* **47**, 1576 (1993)
90. J. J. Halliwell and T. Yu, Alternative derivation of the Hu-Paz-Zhang master equation of quantum Brownian motion, *Phys. Rev. D* **53**, 2012 (1996)
91. R. Karrlein and H. Grabert, Exact time evolution and master equations for the damped harmonic oscillator, *Phys. Rev. E* **55**, 153 (1997)
92. G. W. Ford and R. F. O'Connell, Exact solution of the Hu-Paz-Zhang master equation, *Phys. Rev. D* **64**, 105020 (2001)
93. E. Calzetta, A. Roura, and E. Verdaguer, Master equation for quantum Brownian motion derived by stochastic methods, *Int. J. Theor. Phys.* **40**, 2317 (2001)
94. W. T. Strunz and T. Yu, Convolutionless non-markovian master equations and quantum trajectories: Brownian motion, *Phys. Rev. A* **69**, 052115 (2004)
95. C. Chou, T. Yu, and B. L. Hu, Exact master equation and quantum decoherence of two coupled harmonic oscillators in a general environment, *Phys. Rev. E* **77**, 011112 (2008)
96. C. Chou, B. Hu, and T. Yu, Quantum Brownian motion of a macroscopic object in a general environment, *Physica A* **387**, 432 (2008)
97. R. Xu, B. Tian, J. Xu, and Y. Yan, Exact dynamics of driven Brownian oscillators, *J. Chem. Phys.* **130**, 074107 (2009)
98. P. S. Riseborough, P. Hanggi, and U. Weiss, Exact results for a damped quantum-mechanical harmonic oscillator, *Phys. Rev. A* **31**, 471 (1985)
99. S. Kohler, T. Dittrich, and P. Hänggi, Floquet-Markovian description of the parametrically driven, dissipative harmonic quantum oscillator, *Phys. Rev. E* **55**, 300 (1997)
100. C. Zerbe and P. Hänggi, Brownian parametric quantum oscillator with dissipation, *Phys. Rev. E* **52**, 1533 (1995)
101. H. Li, J. Shao, and S. Wang, Derivation of exact master equation with stochastic description: Dissipative harmonic oscillator, *Phys. Rev. E* **84**, 051112 (2011)
102. J. T. Stockburger, Simulating spin-boson dynamics with stochastic Liouville-von Neumann equations, *Chem. Phys.* **296**, 159 (2004)
103. C. Meier and D. J. Tannor, Non-Markovian evolution of the density operator in the presence of strong laser fields, *J. Chem. Phys.* **111**, 3365 (1999)
104. C. Kreisbeck and T. Kramer, Long-lived electronic coherence in dissipative exciton dynamics of light-harvesting complexes, *J. Phys. Chem. Lett.* **3**, 2828 (2012)
105. V. Shapiro and V. Loginov, Formulae of differentiation and their use for solving stochastic equations, *Physica A* **91**, 563 (1978)
106. Y. Tanimura and R. Kubo, Time evolution of a quantum system in contact with a nearly gaussian-markoffian noise bath, *J. Phys. Soc. Japan* **58**, 101 (1989)
107. Y. Tanimura, Nonperturbative expansion method for a quantum system coupled to a harmonic-oscillator bath, *Phys. Rev. A* **41**, 6676 (1990)
108. Y. Zhou, Y. Yan, and J. Shao, Stochastic simulation of quantum dissipative dynamics, *Europhys. Lett.* **72**, 334 (2005)
109. Z. Tang, X. Ouyang, Z. Gong, H. Wang, and J. Wu, Extended hierarchy equation of motion for the spin-boson model, *J. Chem. Phys.* **143**, 224112 (2015)
110. J. Jin, X. Zheng, and Y. Yan, Exact dynamics of dissipative electronic systems and quantum transport: Hierarchical equations of motion approach, *J. Chem. Phys.* **128**, 234703 (2008)
111. Q. Shi, L. Chen, G. Nan, R.-X. Xu, and Y. Yan, Ef-

ficient hierarchical liouville space propagator to quantum dissipative dynamics, *J. Chem. Phys.* **130**, 084105 (2009)
112. J. Hu, R.-X. Xu, and Y. Yan, Padé spectrum decomposition of fermi function and bose function, *J. Chem. Phys.* **133**, 101106 (2010)
113. K.-B. Zhu, R.-X. Xu, H. Y. Zhang, J. Hu, and Y. J. Yan, Hierarchical dynamics of correlated system-environment coherence and optical spectroscopy, *J. Phys. Chem. B* **115**, 5678 (2011)
114. D. Alonso and I. de Vega, Hierarchy of equations of multiple-time correlation functions, *Phys. Rev. A* **75**, 052108 (2007)
115. M. Sarovar and M. D. Grace, Reduced equations of motion for quantum systems driven by diffusive markov processes, *Phys. Rev. Lett.* **109**, 130401 (2012)
116. I. de Vega, On the structure of the master equation for a two-level system coupled to a thermal bath, *J. Phys. A* **48**, 145202 (2015)
117. Z. Zhou, M. Chen, T. Yu, and J. Q. You, Quantum Langevin approach for non-Markovian quantum dynamics of the spin-boson model, *Phys. Rev. A* **93**, 022105 (2016)
118. A. Ishizaki and G. R. Fleming, Theoretical examination of quantum coherence in a photosynthetic system at physiological temperature, *Proc. Nat. Acad. Sci.* **106**, 17255 (2009)
119. Y.-A. Yan and O. Kühn, Laser control of dissipative two-exciton dynamics in molecular aggregates, *New J. Phys.* **14**, 105004 (2012)
120. Y.-A. Yan and S. Cai, Exciton seebeck effect in molecular systems, *J. Chem. Phys.* **141**, 054105 (2014)
121. Y. Yan, Exciton interference revealed by energy dependent exciton transfer rate for ring-structured molecular systems, *J. Chem. Phys.* **144**, 024305 (2016)
122. L. Chen, R. Zheng, Q. Shi, and Y. Yan, Two-dimensional electronic spectra from the hierarchical equations of motion method: Application to model dimers, *J. Chem. Phys.* **132**, 024505 (2010)
123. X. Zheng, Y. Yan, and M. Di Ventra, Kondo memory in driven strongly correlated quantum dots, *Phys. Rev. Lett.* **111**, 086601 (2013)
124. S. Chakravarty and A. J. Leggett, Dynamics of the two-state system with Ohmic dissipation, *Phys. Rev. Lett.* **52**, 5 (1984)
125. Y. Zhou and J. Shao, Solving the spin-boson model of strong dissipation with flexible random-deterministic scheme, *J. Chem. Phys.* **128**, 034106 (2008)
126. F. Lesage and H. Saleur, Boundary interaction changing operators and dynamical correlations in quantum impurity problems, *Phys. Rev. Lett.* **80**, 4370 (1998)
127. G. M. Whitesides, Reinventing chemistry, *Angew. Chem. Int. Ed.* **54**, 3196 (2015)
128. H. Primas, *Chemistry, Quantum Mechanics and Reductionism: Perspectives in Theoretical Chemistry*, Lecture Notes in Chemistry (Springer, Berlin, 1983)